

Characterisation of forkhead box protein A3 as a key transcription factor for hepatocyte regeneration

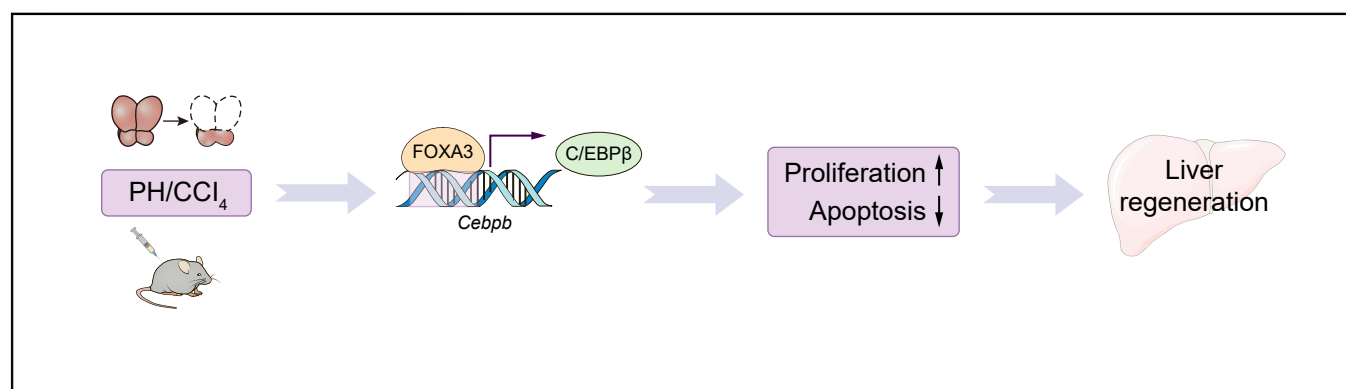
Authors

Guoqiang Li, Lijun Zhu, Mingwei Guo, Dongmei Wang, Meiyao Meng, Yinzhaohong, Zhijian Zhang, Yi Lin, Caizhi Liu, Jiawen Wang, Yahui Zhang, Yining Gao, Yuxiang Cao, Zhirui Xia, Jin Qiu, Yu Li, Shuang Liu, Haibing Chen, Wenyue Liu, Yu Han, Minghua Zheng, Xinran Ma, Lingyan Xu

Correspondence

lyxu@bio.ecnu.edu.cn (L. Xu), xrma@bio.ecnu.edu.cn (X. Ma), zhengmh@wmu.edu.cn (M. Zheng).

Graphical abstract



Highlights

- FOXA3 was induced in an acute hepatocyte proliferation model after partial hepatectomy or CCl₄ administration.
- FOXA3 overexpression or deficiency affected hepatocyte proliferation and apoptosis.
- FOXA3 promotes liver regeneration by regulating the transcription of Cebpb.
- FOXA3 pharmacological inducer cardamonin promotes hepatocyte proliferation without affecting termination after partial hepatectomy.

Impact and Implications

Liver regeneration is vital for the recovery of liver function after chemical insults or hepatectomy, yet the underlying mechanism remains to be elucidated. Herein, via *in vitro* and *in vivo* models and analysis, we demonstrated that Forkhead box protein A3 (FOXA3), a Forkhead box family member, maintained normal liver regeneration progression by governing *Cebpb* transcription and proposed cardamonin as a lead compound to induce Foxa3 and accelerate liver repair, which signified that FOXA3 may be a potential therapeutic target for further preclinical study on treating liver injury.



Characterisation of forkhead box protein A3 as a key transcription factor for hepatocyte regeneration

Guoqiang Li,^{1,†} Lijun Zhu,^{1,†} Mingwei Guo,^{1,†} Dongmei Wang,¹ Meiyao Meng,¹ Yinzhaoyong,¹ Zhijian Zhang,² Yi Lin,² Caizhi Liu,^{1,3} Jiawen Wang,¹ Yahui Zhang,² Yining Gao,³ Yuxiang Cao,¹ Zhirui Xia,¹ Jin Qiu,¹ Yu Li,^{1,4} Shuang Liu,¹ Haibing Chen,^{3,5} Wenyue Liu,⁶ Yu Han,⁴ Minghua Zheng,^{7,8,*} Xinran Ma,^{1,9,10,*} Lingyan Xu^{1,*}

¹Shanghai Key Laboratory of Regulatory Biology, Institute of Biomedical Sciences and School of Life Sciences, East China Normal University, Shanghai, China; ²Department of Endocrinology and Metabolism, Shanghai General Hospital, Shanghai Jiao Tong University of Medicine, Shanghai, China; ³Department of Endocrinology and Metabolism, Shanghai Sixth People's Hospital Affiliated to Shanghai Jiao Tong University School of Medicine, Shanghai, China; ⁴Department of Gastrointestinal Surgery, the First Affiliated Hospital of Wenzhou Medical University, Wenzhou, China; ⁵Department of Endocrinology and Metabolism, Shanghai Tenth People's Hospital, School of Medicine, Tongji University, Shanghai, China; ⁶Department of Endocrinology, the First Affiliated Hospital of Wenzhou Medical University, Wenzhou, China; ⁷MAFLD Research Center, Department of Hepatology, the First Affiliated Hospital of Wenzhou Medical University, Wenzhou, China; ⁸Key Laboratory of Diagnosis and Treatment for The Development of Chronic Liver Disease in Zhejiang Province, Wenzhou, China; ⁹Shanghai Frontiers Science Center of Genome Editing and Cell Therapy, Shanghai Key Laboratory of Regulatory Biology and School of Life Sciences, East China Normal University, Shanghai, China; ¹⁰Chongqing Key Laboratory of Precision Optics, Chongqing Institute of East China Normal University, Chongqing, China

JHEP Reports 2023. <https://doi.org/10.1016/j.jhepr.2023.100906>

Background & Aims: Liver regeneration is vital for the recovery of liver function after injury, yet the underlying mechanism remains to be elucidated. Forkhead box protein A3 (FOXA3), a member of the forkhead box family, plays important roles in endoplasmic reticulum stress sensing, and lipid and glucose homeostasis, yet its functions in liver regeneration are unknown.

Methods: Here, we explored whether Foxa3 regulates liver regeneration via acute and chronic liver injury mice models. We further characterised the molecular mechanism by chromatin immunoprecipitation sequencing and rescue experiments *in vivo* and *in vitro*. Then, we assessed the impact of Foxa3 pharmacological activation on progression and termination of liver regeneration. Finally, we confirmed the Foxa3–Cebpb axis in human liver samples.

Results: Foxa3 is dominantly expressed in hepatocytes and cholangiocytes and is induced upon partial hepatectomy (PH) or carbon tetrachloride (CCl₄) administration. Foxa3 deficiency in mice decreased cyclin gene levels and delayed liver regeneration after PH, or acute or chronic i.p. CCl₄ injection. Conversely, hepatocyte-specific Foxa3 overexpression accelerated hepatocytes proliferation and attenuated liver damage in an CCl₄-induced acute model. Mechanistically, Foxa3 directly regulates Cebpb transcription, which is involved in hepatocyte division and apoptosis both *in vivo* and *in vitro*. Of note, Cebpb overexpression in livers of Foxa3-deficient mice rescued their defects in cell proliferation and regeneration upon CCl₄ treatment. In addition, pharmacological induction of Foxa3 via cardamonin speeded up hepatocyte proliferation after PH, without interfering with liver regeneration termination. Finally, Cebpb and Ki67 levels had a positive correlation with Foxa3 expression in human chronic disease livers.

Conclusions: These data characterise Foxa3 as a vital regulator of liver regeneration, which may represent an essential factor to maintain liver mass after liver injury by governing Cebpb transcription.

Impact and Implications: Liver regeneration is vital for the recovery of liver function after chemical insults or hepatectomy, yet the underlying mechanism remains to be elucidated. Herein, via *in vitro* and *in vivo* models and analysis, we demonstrated that Forkhead box protein A3 (FOXA3), a Forkhead box family member, maintained normal liver regeneration progression by governing Cebpb transcription and proposed cardamonin as a lead compound to induce Foxa3 and accelerate liver repair, which signified that FOXA3 may be a potential therapeutic target for further preclinical study on treating liver injury.

© 2023 The Author(s). Published by Elsevier B.V. on behalf of European Association for the Study of the Liver (EASL). This is an open access article under the CC BY-NC-ND license (<http://creativecommons.org/licenses/by-nc-nd/4.0/>).

Keywords: Liver regeneration; Partial hepatectomy; Carbon tetrachloride; Proliferation; Forkhead box A.

Received 18 December 2022; received in revised form 7 August 2023; accepted 24 August 2023; available online 12 September 2023

[†] These authors contributed equally to this work.

* Corresponding authors. Addresses: Shanghai Key Laboratory of Regulatory Biology, Institute of Biomedical Sciences and School of Life Sciences, East China Normal University, 500 Dongchuan Road, Minhang District, Shanghai, 200241, China. Tel.: +86-021-24206534; Fax: +86-021-24206534 (L. Xu); Shanghai Key Laboratory of Regulatory Biology, Institute of Biomedical Sciences and School of Life Sciences, East China Normal University, 500 Dongchuan Road, Minhang District, Shanghai, 200241, China. Tel.: +86 021-33503359; Fax: +86 021-33503359 (X. Ma); MAFLD Research Center, Department of Hepatology, The First Affiliated Hospital of Wenzhou Medical University, No. 2 Fuxue Lane, Wenzhou, Zhejiang Province, 325000, China. Tel.: +86 577-55579611; Fax: +86 577-55578522 (M. Zheng).

E-mail addresses: lyxu@bio.ecnu.edu.cn (L. Xu), xrma@bio.ecnu.edu.cn (X. Ma), zhengmh@wmu.edu.cn (M. Zheng).



Introduction

The liver plays vital roles in glucose, protein, and lipid metabolism; bile acid synthesis and secretion; endogenous and xenobiotic toxin detoxification; and immune functionality maintenance. Thus, it is central to systematic homeostasis.¹ Profound liver injury is frequent in clinics owing to severe trauma or a high prevalence of liver diseases worldwide, that is, non-alcoholic steatohepatitis (NASH), cirrhosis, or primary liver cancer, which disrupts normal liver functions and can be life-threatening.² Notably, the liver has the unique capability of robust regeneration upon injury.³ Although hepatocyte proliferation is rare in normal adult livers, in scenarios such as hepatitis virus or poison/drug-induced liver injury, or surgical removal caused by liver trauma or primary liver cancer, significant loss of liver mass induces liver regeneration, whereas quiescent hepatocytes re-enter the cell cycle and proliferate to restore liver mass and function under a highly controlled fashion until the liver reaches its normal size.^{4–6} There are key differences in liver regeneration in normal livers with partial hepatectomy (PH) and in diseased livers with massive necrosis and chronic liver diseases. After acute liver injury or hepatectomy, regeneration occurs mainly through hepatocyte replication, whereas in severe liver injury, mature hepatocytes undergo telomere shortening and replicative senescence, which causes cell cycle arrest in hepatocytes.^{7–9} This impairs hepatocyte proliferation and causes hepatocyte apoptosis and necrosis.^{10–12} Therefore, in chronic liver diseases, where hepatocytes experience senescence, new hepatocytes are majorly derived from the activation of cholangiocytes and stem cells.^{13,14}

Avenues to stimulate liver regeneration have long been implicated in clinic to treat patients with massive liver injury. For example, PH is currently the major clinical strategy for primary liver cancer treatment, whereas liver transplantation is the only curative treatment for acute liver failure and end-stage liver disease.¹⁵ Following PH or liver transplantation, the liver undergoes an active and well-controlled phase of liver regeneration to restore its innate mass and function.³ In rodents, PH and carbon tetrachloride (CCl₄) administration are widely used strategies to establish a liver regeneration model. After PH, hepatocytes divide in a relatively synchronous manner, and liver mass and function are restored within 2 weeks.^{4–6} Meanwhile, CCl₄ administration leads to parenchymal necrosis dominantly surrounding the central veins that peaks at 24 h, followed by liver regeneration.^{5,16} As liver regeneration is a complex and sophisticated tissue recovery process, various factors and pathways have been shown to play important roles in it, including hepatocyte growth factors; CCAAT/enhancer-binding protein (C/EBP) family proteins; epidermal/endothelial growth factors and their receptors; and the IL-6–signal transducer and activator of transcription 3 (STAT3), Hippo/Yap, and Wnt/ β -catenin signalling pathways.^{4–6} Because surgically activated liver regeneration, that is, by PH or liver transplantation, is highly dependent on individual physiological conditions or donor tissue availability,^{3–6,15,16} it is desirable to use factors or pathways involved in this process to activate liver regeneration directly. However, proliferation and tumorigenesis are two sides of the same coin; there is concern that the increased proliferation potential of hepatocytes during liver reparations may lose control, therefore favouring carcinogenesis and primary liver cancer.¹⁷ Thus, novel clinical therapeutic targets for safe and efficient activation of liver regeneration to treat liver injury are still in urgent demand.

The Forkhead box A (FOXA) transcription factor (also known as hepatocyte nuclear factor 3 [HNF3]) family comprises three members, namely, Foxa1, Foxa2, and Foxa3, that are involved in multiple physiological events critical in metabolic homeostasis and ageing.^{18,19} Among them, Foxa1 and Foxa2 are essential for liver development as loss of Foxa1 and Foxa2 in the foregut endoderm leads to abrogated hepatic specification in mice.²⁰ By contrast, forkhead box protein A3 (FOXA3), also termed as hepatocyte nuclear factor 3 γ (HNF3 γ), is dispensable for liver development as FOXA3-deficient mice show no defect in liver growth.²¹ However, FOXA3 is the most highly expressed FOXA family member in adult liver, suggesting that it may play roles different from those of Foxa1 and Foxa2 in the liver.^{22,23} For example, we and others have shown that FOXA3 plays crucial roles in lipid and glucose homeostasis in the liver and other metabolic tissues.^{24–27} Importantly, it was reported that FOXA3 level was downregulated in patients with hepatocellular carcinoma (HCC) and inversely correlated with HCC malignancy and patient survival.²⁸ FOXA3 overexpression suppressed HCC growth and sensitised HCC cells to anticancer treatment.²⁸ In addition, FOXA3, synergistically with hepatocyte nuclear factor 1A (HNF1A) and hepatocyte nuclear factor 4A (HNF4A), programmes HCC cells to hepatocyte-like cells,²⁹ overall suggesting that FOXA3 suppresses HCC progression. However, the exact role and detailed mechanism of FOXA3 in acute liver injury and liver regeneration, as well as its targeting strategies, are largely unknown.

In the present study, we demonstrated that FOXA3 plays a critical role in liver regeneration. Ablation of FOXA3 in mice impaired hepatocyte proliferation and exacerbated liver injury, whereas overexpression of FOXA3 promoted liver regeneration and attenuated hepatocyte damage under PH and CCl₄ administration. Mechanistically, via combination of RNA sequencing (RNA-seq) and chromatin immunoprecipitation sequencing (ChIP-seq), we revealed that FOXA3-regulated liver regeneration by governing *Cebpb* transcription and expressing of CCAAT/enhancer-binding protein beta (C/EBP β) through adenoviral delivery in the liver reversed exacerbated liver injury of FOXA3-null mice after CCl₄ treatment. In addition, the active gradient of *Alpinia katsumadai* cardamomin (CDN) is a Foxa3 transcriptional activator and attenuates injury after PH, without interfering with liver regeneration termination. Taken together, our findings provide genetic evidence that FOXA3 regulates liver regeneration and inducing Foxa3 with CDN may be beneficial for treating liver injury.

Materials and methods

Animal and human samples

Male C57BL/6 mice at 8 weeks of age were purchased from GemPharmatech Co., Ltd. (Shanghai, China). FOXA3 wild-type (WT) and knockout (KO) mice were described previously.³⁰ All mice were maintained under a 12-h/12-h light/dark cycle at controlled temperature with *ad libitum* access to food and water. All animal experiment protocols were approved by the ethics committee of Animal Experiments of East China Normal University. For the PH model, two-thirds of the mice liver was removed as previously reported.³¹ Briefly, mice were anaesthetised by gas anaesthesia using 5% isoflurane for induction and 1.5% isoflurane for maintenance. A ventral midline incision was performed to expose the abdominal cavity. Then, the median and

left lateral hepatic lobes were exteriorised. The mice were then ligated and sterilised with betadine after closing the abdominal cavity on a warming pad setting at 37 °C for recovery. For acute liver injury, mice were injected i.p. with control solvent (olive oil) or with CCl₄ (dissolved at 1:9 in olive oil) with the final dose of 1 ml/kg body weight for acute treatment or with the final dose of 0.25 ml/kg body weight for chronic treatment.³² WT and FOXA3 KO mice were treated with CDN (TargetMol, Shanghai, China) at 10 mg/kg body weight or solvent (olive oil) once a day for 3 days before surgery. The liver biopsies were collected from 12 patients with NASH. The study of these specimens was approved by the ethics committee of the First Affiliated Hospital of Wenzhou Medical University, and informed consent was obtained from all participants.

RNA-seq and single-cell RNA-seq analysis

For RNA-seq analysis, Gene Expression Omnibus (GEO) data for liver regeneration (GSE133271, GSE70593, and GSE20427) were downloaded from the NCBI, and differentially expressed genes (DEGs) (adjusted $p \leq 0.05$) from three datasets were overlapped using the online tool Draw Venn Diagram (<https://bioinformatics.psb.ugent.be/webtools/venn>). Gene ontology (GO) enrichment analysis of overlapped DEGs was performed using the online webtool DAVID Bioinformatic Resources (2021 update). The significant levels of terms and biological processes were corrected using the p value with a rigorous threshold ($p \leq 0.05$) by Bonferroni correction.

For single-cell RNA sequencing (scRNA-seq) analysis, data from 4,058 non-parenchymal cells (GSE129516) and 3,153 parenchymal cells (GSE157698) from the GEO database were combined. We also re-analysed the scRNA-seq data (GSE162713)³³ to study spatial Foxa3 expression and scRNA-seq data from control and NASH mice (GSE210501) to study correlation of Foxa3 expression with cholangiocytes-derived hepatocytes (Trop2) in mice. The Harmony algorithm (version 1.0) was used for removing batch effects, in which real biological differences are interspersed with technical differences.³⁴ The Seurat package (version 4.1.1; <https://satijalab.org/seurat/>) was used to analyse scRNA-seq data.³⁵ A total of 7,211 cells expressing more than 200 genes (min.features = 200) and 15,478 genes with transcripts detected in more than three cells (min.cells = 3) were used for further analysis. The t-distributed stochastic neighbour embedding (t-SNE) plots and feature plots were generated by R (version 4.2.0, R Foundation for Statistical Computing, Vienna, Austria). The identity of marker genes for each cluster was assigned based on the prior knowledge of marker genes.^{36,37}

Plasmid construction

The FOXA3 expression plasmid and Foxa3-luciferase reporter were constructed as previously described.²⁴ The Cebpb promoter was amplified from mouse genomic DNA and inserted to the pGL3-basic luciferase reporter vector (E1751; Promega, Madison, WI, USA). The mutant Cebpb-luciferase reporter with a deletion at the putative FOXA3 binding site was generated using the QuikChange II Site-Directed Mutagenesis Kit (200523; Agilent, Santa Clara, CA, USA). Primers are listed in Table S1.

Cell culture and treatment

Mouse AML12 cells were cultured with 89% DMEM/F12 (11330-032; Invitrogen, Carlsbad, CA, USA), 10% FBS (10099; Gibco, Grand Island, NY, USA), 1% insulin–transferrin–selenium liquid media supplement (13146; Sigma-Aldrich, St. Louis, MO, USA),

and dexamethasone at 40 ng/ml. For FOXA3 overexpression, AML12 cells were transfected with FOXA3 expression plasmid by using Lipofectamine 2000 Reagent (11668019; Thermo Fisher Scientific, Waltham, MA, USA). For FOXA3 or Cebpb knockdown, AML12 cells were transfected with a negative control small interfering RNA (siRNA) (siNC) or siFOXA3 or siCebpb by using Lipofectamine 2000 Reagent. The sequences of siRNAs were as follows: siNC, 5'-UUCUCCGAACGUGUCACGUTT-3'; siFoxa3, 5'-GGCAUUCGUGUCCUUAATT-3'; and siCebpb, 5'-GCGACGA-GUACAAGAUGCGTT-3' (designed and synthesised by GenePharma, Shanghai, China). AML12 cells were treated with 10 μM CDN (TargetMol) for analysis.

Real-time quantitative PCR

Total RNAs were extracted from livers or cultured cells using TRIzol (9109; Takara Bio, Beijing, China), followed by 500 ng cDNA synthesis using the First Strand cDNA Synthesis Kit (RR036A; Takara, Beijing, China). cDNA samples and specific primers were mixed with SYBR green fluorescent dye and then loaded into a 384-well plate. Real-time quantitative PCR was performed with the Light Cycler 480II detection system (Roche, Basilea, CH, Switzerland). The Gapdh gene was selected as the housekeeping gene. Gene expression levels were assessed using the $\Delta\Delta C_t$ method with triplicates. Primer sequences are listed in Table S2.

Immunoblotting

Total protein was extracted from liver samples or cells by RIPA buffer (P0013B; Beyotime Biotechnology, Shanghai, China) containing protease inhibitors (P1046; Beyotime Biotechnology) and phenylmethylsulfonyl fluoride (ST505; Beyotime Biotechnology) and then placed on ice. Protein concentration was measured by BCA assay (P0012; Beyotime Biotechnology). Protein samples were loaded on Tris-HCl gel in running buffer at 80 V for 2 h. Polyvinylidene difluoride membranes were used to transfer protein at constant voltage (100 V) and then blocked with 10% bovine serum albumin buffer at room temperature. The membranes were then incubated with primary antibodies (Table S3) at 4 °C overnight and then washed with TBST, followed by incubation with IRDye 680RD goat anti-rabbit or IRDye 770RD goat anti-mouse secondary antibodies. The results were imaged using the Odyssey CLx Imager system (LI-COR, Lincoln, NE, USA), and protein expression levels were quantified using Image Studio software (LI-COR).

ALT and AST analysis

To determine serum alanine aminotransferase (ALT) and aspartate aminotransferase (AST) levels, mice blood samples were left overnight at 4 °C and centrifuged at 3,500 rpm/min at 4 °C for 15 min. Serum ALT and AST were measured using commercial enzyme kits (KHB Company, Shanghai, China).

Histological analysis

For H&E staining, liver tissues were fixed with 4% paraformaldehyde, followed by dehydration, transparency, paraffin embedding, and sectioning at 5 μm. The liver sections were stained with the H&E kit (C0105M; Beyotime Biotechnology). For the immunohistochemistry of Ki67 staining, liver sections were blocked with 10% goat serum after 3% H₂O₂ treatment, which was used to quench endogenous peroxidase activity. The primary antibody of Ki67 (ICH-00375, 1:200 dilution; Bethyl) was incubated overnight at 4 °C and then washed with PBS three times,

followed by incubation with goat anti-rabbit IgG (SP-9002; ZSGB-BIO, Beijing, China) and IgG-HRP (SP-9002; ZSGB-BIO). The signal was detected using the DAB kit (SP-9002; ZSGB-BIO). Images were acquired using an Olympus microscope and a Leica SP8 confocal microscope (Leica, Heidelberg, Germany). For immunofluorescence, anti-Ki67 (IHC-00375, 1:200 dilution; Bethyl), anti-pHH3 (53348, 1:200 dilution; CST), and anti-CK19 (TROMA-III, 1:200 dilution; DSHB) were used, followed by DyLight 488/549 goat anti-rabbit secondary antibody and DAPI for nuclear staining, and subsequently mounted with Antifade Mounting Medium (P0126; Beyotime Biotechnology). Images were acquired using a Nikon fluorescence microscope (Nikon, Tokyo, Japan).

TUNEL analysis and immunofluorescence

For terminal deoxynucleotidyl transferase-mediated deoxyuridine triphosphate nick-end labelling (TUNEL) assay, liver sections were dewaxed, rehydrated, and treated with proteinase K (20 µg/ml) for 30 min at 37 °C. TUNEL analysis was performed using the *In situ* Cell Death Detection Kit, TMR red (12156792910; Roche), following the manufacturer's instructions. The TUNEL-positive area was quantified using ImageJ software.

For immunofluorescence, AML12 cells on glass coverslips were fixed with 4% paraformaldehyde, permeabilised, blocked, and incubated with anti-ki67 antibody (IHC-00375, 1:200 dilution; Bethyl), followed by DyLight 488/549 goat anti-rabbit secondary antibody and DAPI for nuclear staining, and subsequently mounted with Antifade Mounting Medium (P0126; Beyotime Biotechnology). Images were acquired using a Nikon fluorescence microscope.

Adenoviral or adeno-associated viral delivery in mouse livers

Adenoviruses expressing murine FOXA3, C/EBPβ, or GFP (Ad-FOXA3, Ad-C/EBPβ, or Ad-GFP, respectively) were generated by Genechem (Shanghai, China). Hepatocyte-specific thyroxine-binding globulin (TBG) promoter-driven adeno-associated viruses expressing FOXA3 or GFP (AAV-TBG-FOXA3 or AAV-TBG-GFP, respectively) were generated by HANBIO (Shanghai, China). Mice were injected with Ad-FOXA3, Ad-C/EBPβ, Ad-GFP (1×10^9 plaque-forming units), or AAV-TBG-FOXA3 or AAV-TBG-GFP (1×10^{11} plaque-forming units) by tail vein injection.

ChIP assays and ChIP-seq

Chromatin immunoprecipitation (ChIP) assays were performed according to the manufacturer's instructions (9003S; Cell Signaling Technology, Danvers, MA, USA). For *in vivo* ChIP, the mouse liver (100 mg) was minced into small pieces, cross-linked with 1% formaldehyde at room temperature for 10 min, and stopped with 0.125 M glycine solution. Unicellular suspension was prepared by Dounce homogenisation in ice-cold PBS. For *in vitro* ChIP, AML12 cells were cross-linked with 1% formaldehyde and then stopped with 0.125 M glycine solution. Cells were collected with SDS lysis buffer after washing with ice-cold PBS. Sonication with a Bioruptor sonicator (Scientz, Ningbo, China) was used to fragment chromatin. Samples were incubated with Protein G Agarose beads and then immunoprecipitated with IgG (2729S; Cell Signaling Technology), anti-FOXA3 antibody (sc-74424; Santa Cruz, Dallas, TX, USA), or anti-histone H3 (acetyl K9) antibody (ab4441; Abcam, Cambridge, UK) overnight at 4 °C. Cross-linking was reversed at 65 °C for 2 h, and DNA fragments were purified for real-time quantitative PCR. The sequences are listed in Table S2.

ChIP-seq was performed by Genergy (Shanghai, China). The construction of libraries and data analysis was described previously.¹⁶ Briefly, at least 100 ng DNA per sample was used to generate libraries using a commercial kit, and then libraries were sequenced on an Illumina HiSeq3000 platform (Illumina, San Diego, CA, USA). For data analysis, sequencing reads were mapped to the mouse reference (mm10) using Bowtie2 (v.2.2.5). MACS2 (v.2.1.1) was used to scan peaks in the genomic-wide level according to each immunoprecipitation and input pair. Visualisation was performed using the Integrative Genomic Viewer (IGV) genome browser (v.2.8.0).

Transfection and luciferase assays

HEK293T and AML12 cells were cultured with 10% FBS (10099; Gibco, Grand Island, NY, USA) and 1% penicillin/streptomycin (15140122; Thermo Fisher Scientific) and transfected with plasmids using EZ cell Transfection Reagent (AC04L091; Life-iLab Biotech, Shanghai, China). For luciferase assay, expression plasmid, reporter plasmid, and pRL-SV40 were co-transfected into HEK293T or AML12 cells. Cells were collected 48 h after transfection, and the relative luciferase activity was assessed using the *TransDetect* Double-Luciferase Reporter Assay Kit (FR201-01; TransGen Biotech, Beijing, China). Commercially available natural compounds were purchased from TargetMol for analysis. Each group was repeated in triplicate.

Flow cytometry analysis of apoptotic cells and cell cycle distribution

AML12 cells were harvested after transfection with siRNAs using Lipofectamine 2000 reagent (11668019; Thermo Fisher Scientific) and washed with ice-cold PBS. For apoptosis analysis, the APC Annexin V Apoptosis Detection Kit with PI (640932; BioLegend, San Diego, CA, USA) was used, and apoptotic cells were quantified using a flow cytometer (BD Fortessa). To measure the cell cycle distribution, cells were fixed in prechilled 70% ethanol for 30 min, followed by staining with propidium iodide solution (C1052; Beyotime Biotechnology; Shanghai, China) and examined using a flow cytometer (BD Fortessa). The data were analysed using FlowJo v.10 software.

Statistics

All experiments were replicated at least three times, and all analyses were performed using GraphPad software (GraphPad, San Diego, CA, USA). Significance between two groups were compared using the Student *t* test. One-way ANOVA was used to compare data from multiple groups. Pearson correlation analysis was used to analyse correlation between two parameters. All data are displayed as mean ± SEM. Significant differences among groups are indicated as **p* < 0.05, ***p* < 0.01, and ###*p* < 0.01.

Results

FOXA3 is specifically expressed in hepatocytes and cholangiocytes and is induced in mouse liver during regeneration

To understand the key regulators involved in liver regeneration, we firstly analysed three RNA-seq datasets (GSE133271, GSE70593, and GSE20427) that compare gene expressions of mice livers with or without PH. A total of 513 DEGs were consistently changed in three GEO datasets (Fig. 1A), among which GO enrichment analysis highlighted transcriptional regulation as the top enriched biological process (Table S4). As

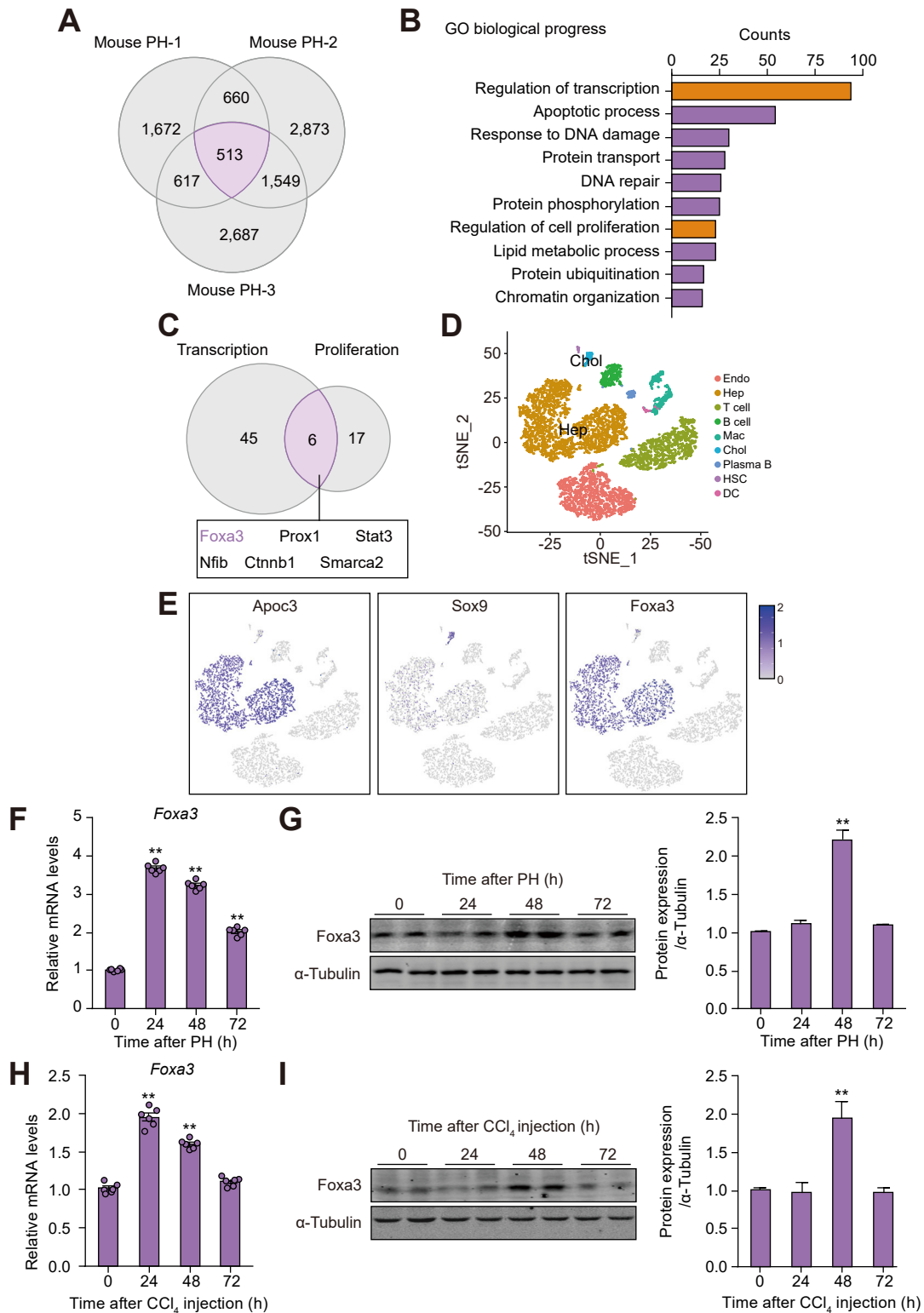


Fig. 1. FOXA3 is specifically expressed in hepatocytes and cholangiocytes and induced in mouse liver regeneration. (A) Venn diagram illustrating overlap of DEGs during liver regeneration among three different RNA-seq datasets (GSE133271, GSE70593, and GSE20427) of mouse PH. (B) Top 10 GO enrichment analysis of the 513 common DEGs. (C) Venn diagram showing the six transcription factors involved in cell proliferation biological process. (D, E) t-SNE visualisation of liver cell cluster, hepatocyte, and cholangiocyte marker genes. Cell clusters are annotated as Endo, Mac, T cells, B cells, DC, Chol, Hep, plasma B cells, and HSC based on the marker genes. (F–I) Expression of hepatic mRNA and protein of FOXA3 at different time after PH or CCl₄ injection. Data are presented as mean ± SEM. Significance was determined using the Student two-tailed *t* test. **p* < 0.05, ***p* < 0.01, as indicated. n = 6 per group. CCl₄, carbon tetrachloride; Chol, cholangiocytes; DC, dendritic cells; DEG, differentially expressed gene; Endo, endothelial cells; FOX3, forkhead box protein A3; GO, gene ontology; Hep, hepatocytes; HSC, hepatic stellate cells; Mac, macrophages; PH, partial hepatectomy; RNA-seq, RNA sequencing; t-SNE, t-distributed stochastic neighbour embedding.

hepatocyte proliferation is the most active and important event upon PH, we subsequently overlapped genes enriched in transcription process with genes enriched in cell proliferation process to focus on transcription factors (TFs) governing proliferation, which allowed us to identify six TFs (Foxa3, Prox1, Stat3, Nfib, Ctnnb1, and Smarca2) of potential importance in liver regeneration (Fig. 1B and C). Hepatocytes and cholangiocytes are major origins of proliferated hepatocytes during liver regeneration.^{3–6} Importantly, we found via scRNA-seq analysis that, among the six TFs found, Foxa3 and Prox1 feature high and specific expressions in hepatocytes and cholangiocytes in the liver, whereas Foxa3 features the highest expression among these TFs in hepatocytes and cholangiocytes (Fig. 1D and E, and Fig. S1A and B). Consistent with the preferential expression of Foxa3 in the mature liver,^{22,23} we also found that Foxa3 showed a predominant expression compared with its family members Foxa1 and Foxa2 in hepatocytes and cholangiocytes (Fig. S1C). Considering that Prox1 has been reported to play an oncogenic role in HCC,³⁸ whereas Foxa3 has been shown to suppress HCC, we next focused on unravelling the function of Foxa3 in liver regeneration.

Furthermore, we also analysed the spatial Foxa3 expression via scRNA-seq data (GSE162713) and found that Foxa3 was equally expressed in zone 1, 2, and 3 hepatocytes. Considering midlobular zone 2 hepatocytes have been reported as the main source of hepatocyte regeneration,³³ our finding suggested that FOXA3 at least partially respond to liver injury (Fig. S1D and E).

We performed PH or CCl₄ administration in C57BL/6J mice to induce acute hepatocyte proliferation and studied the dynamics of Foxa3 expression in the liver. Interestingly, we found that hepatic Foxa3 mRNA levels and protein levels peaked 24 and 48 h, respectively, after PH or CCl₄ injection, and gradually dropped after 72 h, suggesting that FOXA3 may play an active role in liver regeneration (Fig. 1F and G).

Loss of FOXA3 in mice delays liver regeneration after PH

We then take advantage of genetic animal models and subjected WT and FOXA3 KO mice to PH surgery and analysed livers 48, 168, and 336 h post PH to investigate the role of FOXA3 in liver regeneration (Fig. 2A). Compared with WT, FOXA3 deficiency in mice impaired hepatocyte proliferation after PH, as evidenced by decreased mitotic hepatocytes and Ki67-positive cells shown in H&E and immunohistochemistry staining, as well as subdued liver regeneration, as shown by increased serum levels of ALT and AST, and lower liver/body weight ratio 48 h after PH. However, these parameters were reversed 168 h after injury, and WT and FOXA3 KO mice performed similarly 336 h after PH (Fig. 2B–H and Fig. S2C). These were not attributable to a basal difference between WT and FOXA3 mice, as they have comparable liver weights and serum parameters at baseline (Fig. 2B, C, and H). Thus, these data suggested that loss of FOXA3 worsened hepatic injury and delayed liver mass restoration.

Considering the vital roles of cell cycle activation in hepatocyte proliferation and liver regeneration,³ we examined expression levels of various cyclins controlling different cell cycle phases. Compared with the robust induction of cell cycle genes in WT mice upon PH, FOXA3 KO mice had significantly blunted mRNA levels of Cyclin A1, Cyclin B1, Cyclin B2, and Cyclin E, as well as protein levels of Cyclin A, Cyclin B1, and total cyclin-dependent kinase (CDK) in the liver, as shown by real-time quantitative PCR and immunoblotting at 48 h, but reversed at 168 h and were similar at 336 h after PH in a comparable fashion

of liver repair parameters (Fig. 2H–L and Fig. S2A). The delayed regeneration in FOXA3 KO mice at 48 h after PH may partially be as a result of changes in a direct mitogen of hepatocytes, as epidermal growth factor (EGF) and hepatocyte growth factor (HGF) levels were lower in FOXA3 KO mice than in WT mice (Fig. S2B). Together, these data demonstrated that loss of FOXA3 resulted in decreased capacity of hepatocytes to re-enter the cell cycle for cell proliferation, which may underline the defects of FOXA3 KO mice in engaging hepatocyte proliferation and delayed restoration to their original liver mass after PH.

Ablation of FOXA3 in mice exacerbates CCl₄-induced hepatocyte damages and delays liver regeneration

CCl₄ imposes chemical damage to the liver, which induces acute liver injury and subsequent hepatocyte proliferation and liver regeneration.^{5,16,32} We further established a CCl₄-induced liver damage model by i.p. administration of CCl₄ in WT and FOXA3 KO mice and examined liver samples 24, 48, 96, and 168 h afterwards (Fig. 3A). Consistent with the PH model, FOXA3-deficient mice also exhibited decreased Ki67 immunohistochemistry staining, exacerbated lobular necrosis and apoptotic TUNEL-positive cells, and increased serum ALT and AST levels 24 and 48 h after CCl₄ administration, whereas these parameters were largely reversed after 96 h and became similar between WT and FOXA3 KO mice 168 h post chemical insult (Fig. 3B–H). Meanwhile, molecular analysis showed similar patterns in mRNA levels of cyclin genes including Cyclin A1, Cyclin B1, Cyclin B2, and Cyclin E, as well as protein levels of Cyclin A, Cyclin B1, and total CDK (Fig. 3I–L and Fig. S3A). Consistent with the PH model, the hepatic mitogen HGF and EGF levels were decreased in FOXA3 KO mice (Fig. S3B). In addition, liver metabolic activity as shown by levels of CYP family members were similar between WT and FOXA3 KO mice (Fig. S3C). The decreases in expressions of cell cycle genes are not attributable to a defect of FOXA3-deficient cells to enter various stages of cell cycles, as FOXA3 knockdown in hepatocytes did not significantly change overall cell cycle distribution (Fig. S3D and E). In addition, we found that the impacts of FOXA3 on cell proliferation and apoptosis are hepatocyte-autonomous, as Foxa3 knockdown blunted Ki67 levels and caused defective cell mitosis in hepatocyte cell line AML12 (Fig. S3F), as well as led to increased apoptosis as shown by FACS analysis of Annexin V (Fig. S3G). Together, these data suggested that ablation of FOXA3 exacerbated apoptosis and inhibited proliferation, which led to incompetent recovery in response to CCl₄ treatment.

Overexpression of FOXA3 in liver promotes hepatocyte proliferation and attenuates liver injury induced by CCl₄

Conversely, to investigate whether FOXA3 overexpression promotes liver regeneration, adenovirus-mediated control (Ad-GFP) or FOXA3 (Ad-FOXA3) delivery in liver was achieved via mice tail vein injection followed by CCl₄ treatment (Fig. S4A). Indeed, we found that FOXA3 overexpression enhanced hepatocyte proliferation as shown by increased Ki67 staining, as well as decreased hepatocyte necrosis as shown in H&E staining and TUNEL-positive cells (Fig. S4B–D). Moreover, significant reduction of serum ALT and AST levels suggested better recovery of Ad-FOXA3 mice upon CCl₄-induced liver injury (Fig. S4E). Molecular analysis further showed that FOXA3 overexpression enhanced the expressions of cell cycle genes in mice livers treated with CCl₄ (Fig. S4F). Immunoblot analysis also revealed enhanced Cyclin A, Cyclin B1, and total CDK protein levels in livers of mice treated

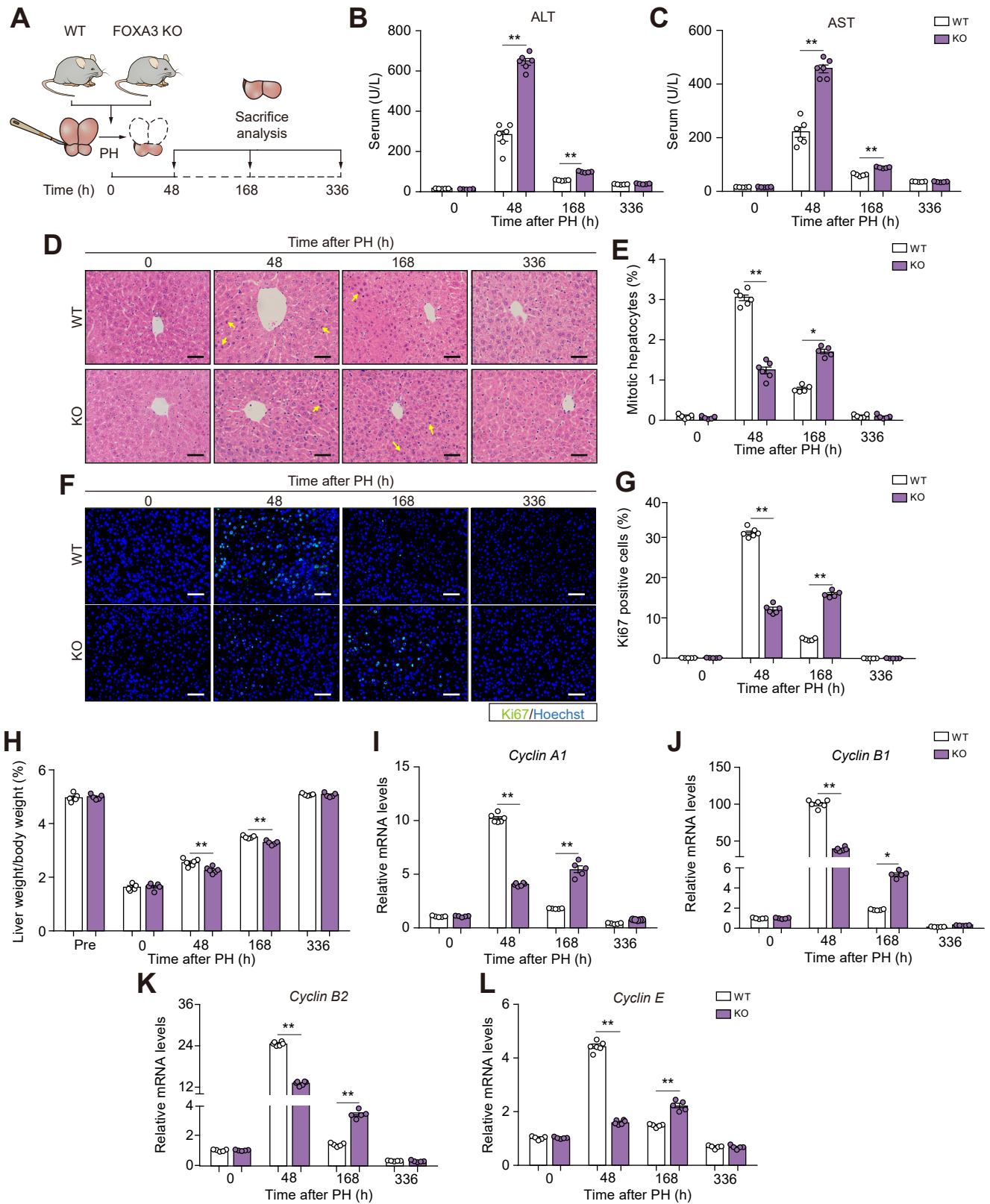


Fig. 2. Loss of FOXA3 in mice impairs liver regeneration after PH. (A) WT and FOXA3 KO mice were subjected to PH. (B, C) Serum ALT and AST levels 48, 168, and 336 h after PH. (D, E) Representative H&E staining of liver sections, and the mitotic hepatocytes were quantified 48, 168, and 336 h after PH. (F, G) Immunofluorescence of liver sections for Ki67 48, 168, and 336 h after PH and Ki67-positive cells were quantified. (H) Liver weight relative to body weight was determined 48, 168, and 336 h after PH. (I–L) Hepatic expression of cell cycle genes 48, 168, and 336 h after PH. Data are presented as mean ± SEM. Significance was determined using the Student two-tailed *t* test. **p* < 0.05, ***p* < 0.01, as indicated. Scale bar, 50 μm. n = 6 per group. ALT, alanine aminotransferase; AST, aspartate aminotransferase; FOXA3, forkhead box protein A3; KO, knockout; PH, partial hepatectomy; WT, wild-type.

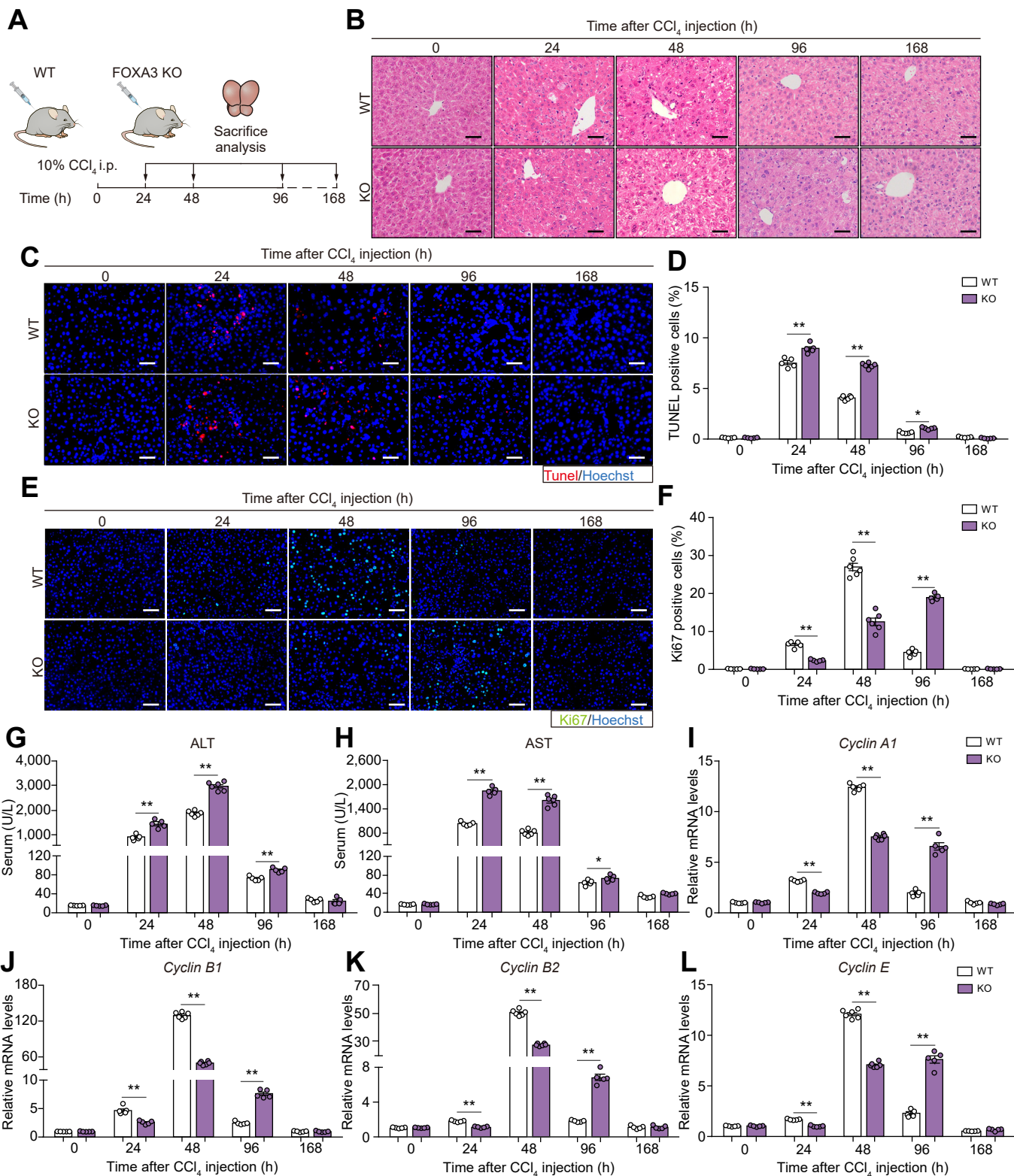


Fig. 3. Ablation of FOXA3 in mice exacerbates CCl₄-induced hepatocyte damage and decreases liver regeneration. (A) WT and FOXA3 KO mice treated with CCl₄ (1 ml/kg body weight, i.p.) or olive oil. (B–D) Representative H&E staining and TUNEL staining of liver sections 24, 48, 96, and 168 h after CCl₄ injection. (E, F) Immunofluorescence of liver sections for Ki67 24, 48, 96, and 168 h after CCl₄ injection, and Ki67-positive cells were quantified. (G, H) Serum ALT and AST levels 24, 48, 96, and 168 h after CCl₄ injection. (I–L) Hepatic expression of cell cycle genes 24, 48, 96, and 168 h after CCl₄ injection. Data are presented as mean ± SEM. Significance was determined using the Student two-tailed *t* test. **p* < 0.05, ***p* < 0.01, as indicated. Scale bar, 50 μm. *n* = 6 per group. ALT, alanine aminotransferase; AST, aspartate aminotransferase; CCl₄, carbon tetrachloride; FOXA3, forkhead box protein A3; TUNEL, terminal deoxynucleotidyl transferase-mediated deoxy-uridine triphosphate nick-end labelling.

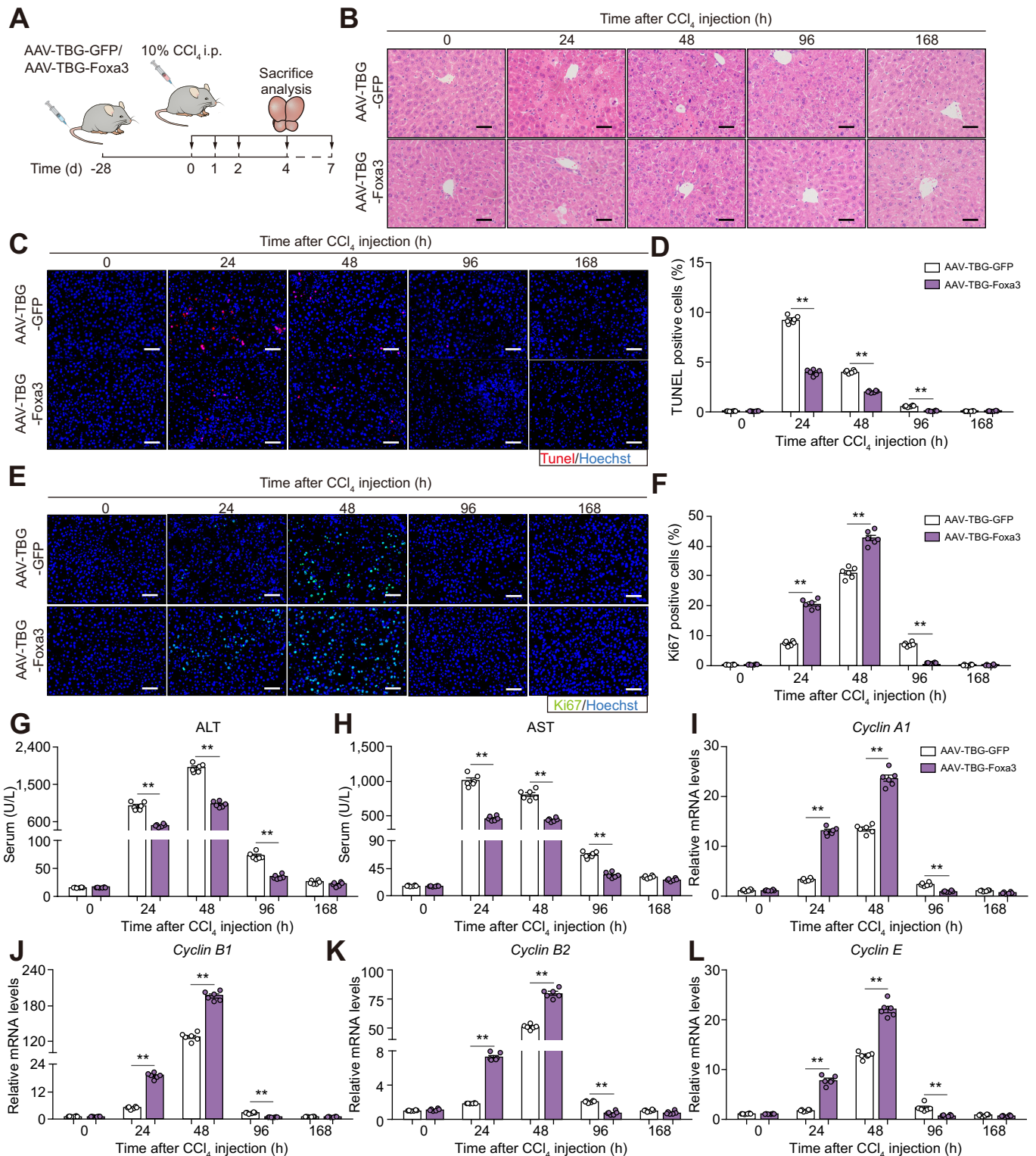


Fig. 4. Hepatocyte-specific overexpression of Foxa3 accelerates liver regeneration and attenuates liver injury induced by CCl₄. (A) Twenty-eight days after a tail vein injection with AAV-TBG-GFP or AAV-TBG-Foxa3, C57BL/6 mice were treated with CCl₄ (1 ml/kg body weight, i.p.). (B–D) Representative H&E staining and TUNEL staining of liver sections 24, 48, 96, and 168 h after CCl₄ injection. (E, F) Immunofluorescence of liver sections for Ki67 24, 48, 96, and 168 h after CCl₄ injection, and Ki67-positive cells were quantified. (G, H) Serum ALT and AST levels 24, 48, 96, and 168 h after CCl₄ injection. (I–L) Hepatic expression of cell cycle genes 24, 48, 96, and 168 h after CCl₄ injection. Data are presented as mean ± SEM. Significance was determined using the Student two-tailed *t* test. **p* < 0.05, ***p* < 0.01, as indicated. Scale bar, 50 μm. *n* = 6 per group. AAV, adeno-associated virus; ALT, alanine aminotransferase; AST, aspartate aminotransferase; CCl₄, carbon tetrachloride; FOXA3, forkhead box protein A3; GFP, green fluorescent protein; TBG, thyroxine-binding globulin; TUNEL, terminal deoxynucleotidyl transferase-mediated deoxyuridine triphosphate nick-end labelling.

with CCl₄ compared with control mice (Fig. S4G). These results demonstrated that mice with hepatic FOXA3 overexpression were resistant to chemical-induced liver injury.

Furthermore, aside from hepatocytes, cholangiocytes and liver stem cells have been reported to also contribute substantially to liver regeneration in various pathological conditions.^{13,14} To emphasise the role of hepatocyte FOXA3 in liver repair, we established a hepatocyte-specific FOXA3 overexpression mice model via AAV-TBG-FOXA3 injection (Fig. S5A) and examined livers from hepatocyte-specific FOXA3 overexpression (AAV-TBG-FOXA3) mice and control (AAV-TBG-GFP) mice 24, 48, 96, and 168 h after CCl₄ treatment (Fig. 4A). We found that AAV-TBG-FOXA3 administration in mice promoted liver repair as demonstrated by improved liver histological analysis, decreased apoptosis in TUNEL analysis, enhanced proliferation marker Ki67 expression, reduced serum ALT and AST levels, and increased hepatic cyclin gene expressions both 24 and 48 h after CCl₄ treatment (Fig. 4B–L and Fig. S5B). These parameters were reversed 96 h after treatment, but both groups behaved similarly 168 h after liver injury (Fig. 4B–L and Fig. S5B). As expected, levels of HGF and EGF were increased in AAV-TBG-FOXA3 mice, whereas CYP family members were similar between AAV-TBG-FOXA3 and control mice (Fig. S5C and D). Of note, AAV-TBG-FOXA3 treatment without CCl₄ injection showed no difference in liver weights and cyclin gene expressions, suggesting that overexpression of *Foxa3* does not cause hepatomegaly or hepatocyte proliferation in healthy livers (Fig. S5E and F). These results showed that specific FOXA3 overexpression in hepatocytes accelerated liver regeneration in mice.

Ablation of FOXA3 in mice exacerbates chronic CCl₄ administration-induced liver injury and delayed regeneration

In chronic liver diseases where hepatocytes undergo extensive senescence and their ability to enter the cell cycle for proliferation are severely impaired, cholangiocytes and liver stem cells contributed greatly to newly formed hepatocytes.^{7–9,13,14} Therefore, to study the possible contribution of FOXA3 in cholangiocytes toward the repair process in chronic liver disease, we established a chronic liver injury model, where WT and FOXA3 KO mice were subjected to 4-week CCl₄ injection and recovered for 1, 7, or 14 days (Fig. S6A). We found that *Foxa3* deficiency promoted cellular senescence (Fig. S6B and C), as well as delayed cell proliferation and liver damage recovery, in this chronic liver injury model, as liver damages were more severe in FOXA3 KO mice after 1- and 7-day recovery compared with WT mice and only reversed after 14-day recovery when WT mice were largely restored (Fig. S6D–J). We then assessed the impact of FOXA3 deficiency on cholangiocytes during liver regeneration under long-term CCl₄ administration in mice. Indeed, staining of CK19 (a marker for cholangiocytes) suggested that after 1- and 7-day recovery, FOXA3 KO mice featured reduced numbers of cholangiocytes compared with WT mice, whereas subsequently CK19⁺ cells were increased in FOXA3 KO mice after 14-day recovery (Fig. S6K), which were in consistent with the delayed tissue repair in KO mice. These data suggested that, aside from hepatocytes, FOXA3 deficiency also influenced numbers of cholangiocytes, which may possibly contribute to delayed liver regeneration in FOXA3 KO mice.

In addition, we re-analysed scRNA-seq data from control and NASH mice (GSE210501), which demonstrated a positive correlation of *Foxa3* expression with cholangiocyte-derived

hepatocytes (Trop2) in mice (Fig. S7A), suggesting that FOXA3 may also regulate proliferation in cholangiocytes and stem cells. The regulatory roles of cholangiocytes/stem cells FOXA3 in liver regeneration warrant further investigation.

FOXA3 regulates *Cebpb* transcription during liver regeneration

Next, we investigated the mechanism of FOXA3 in the regulation of liver regeneration. Because FOXA3 is a TF, we analysed our in-house FOXA3 ChIP-seq data and identified 457 potential FOXA3 direct target genes.²⁵ We then overlapped the FOXA3 targets from ChIP-seq data with the 513 common DEGs from RNA-seq datasets in Fig. 1A, which revealed 30 genes (Table S5) that exhibit expression changes during liver regeneration progression while under direct FOXA3 regulation (Fig. 5A). Among them, *Cebpb* manifested as the top enriched gene (Fig. 5B). Of note, we obtained 12 liver samples from patients with NASH and found that *Cebpb* and Ki67 mRNA levels were positively correlated with FOXA3 levels in NASH livers, suggesting the regulation of C/EBP β and proliferation by FOXA3 in human samples with chronic liver injury (Fig. S7B and C). Consistent with this, FOXA3 knockdown attenuated but FOXA3 overexpression induced *Cebpb* expression in both mRNA and protein levels in liver cells (Figs. S8A and S9A). Of note, consistent with ChIP-seq data (Fig. 5C), according to *in silico* analysis indicating the existence of a putative FOXA3 binding site on the *Cebpb* promoter (Fig. 5D), ChIP assay confirmed the direct FOXA3 binding on the *Cebpb* promoter (Fig. 5E). Furthermore, luciferase assay indicated that FOXA3 induced *Cebpb* transcription, whereas mutation of the putative FOXA3 binding site abolished this transcription activation (Fig. 5F).

C/EBP β has been reported to contribute to hepatocyte replication and proliferation upon stresses and hepatocyte growth factor stimulation.^{39,40} We found that *Cebpb* mRNA and protein levels were decreased in livers of FOXA3 KO mice compared with WT mice 48 h after both PH and CCl₄ injection (Fig. 5G and H). Conversely, *Cebpb* mRNA and protein expression was increased in hepatic FOXA3 overexpression (Ad-Foxa3) mice vs. control (Ad-GFP) mice 48 h after CCl₄ injection (Fig. 5I). In addition, *Cebpb* levels showed a positive correlation with *Foxa3* levels in livers of mice under regeneration via PH or CCl₄ administration (Fig. 5J). Overall, these data suggested that *Cebpb* is the direct transcriptional target of *Foxa3*. Interestingly, baseline *Cebpb* expression was similar between WT and KO mice or mice treated with Ad-GFP and Ad-Foxa3, suggesting that the regulatory axis of *Foxa3*–*Cebpb* might be initiated upon liver injury (Fig. S7D and E).

We also investigated other possible mechanisms in addition to *Foxa3*–*Cebpb*-mediated hepatocyte proliferation during liver regeneration. GO analysis revealed that *Foxa3* target genes were broadly involved in the regulation of apoptosis, metabolic process, and DNA damage, which were closely related to liver injury and regeneration (Fig. S7F). In addition, the 30 genes overlapped between FOXA3 ChIP-seq targets and common DEGs from RNA-seq of mice livers with or without PH. GO analysis revealed that apoptotic process, DNA damage response, and response to lipopolysaccharide were enriched (Fig. S7G). Interestingly, in addition to *Cebpb*, PH also induced other key transcriptional factors, including *Gr*, *Fxr*, *Yy1*, and *Foxo3*, which are reported to be involved in liver injury, functions, and regeneration.^{41–46} These gene alternations were confirmed in WT and FOXA3 KO mice after acute and chronic liver injuries (Fig. S7H–J).

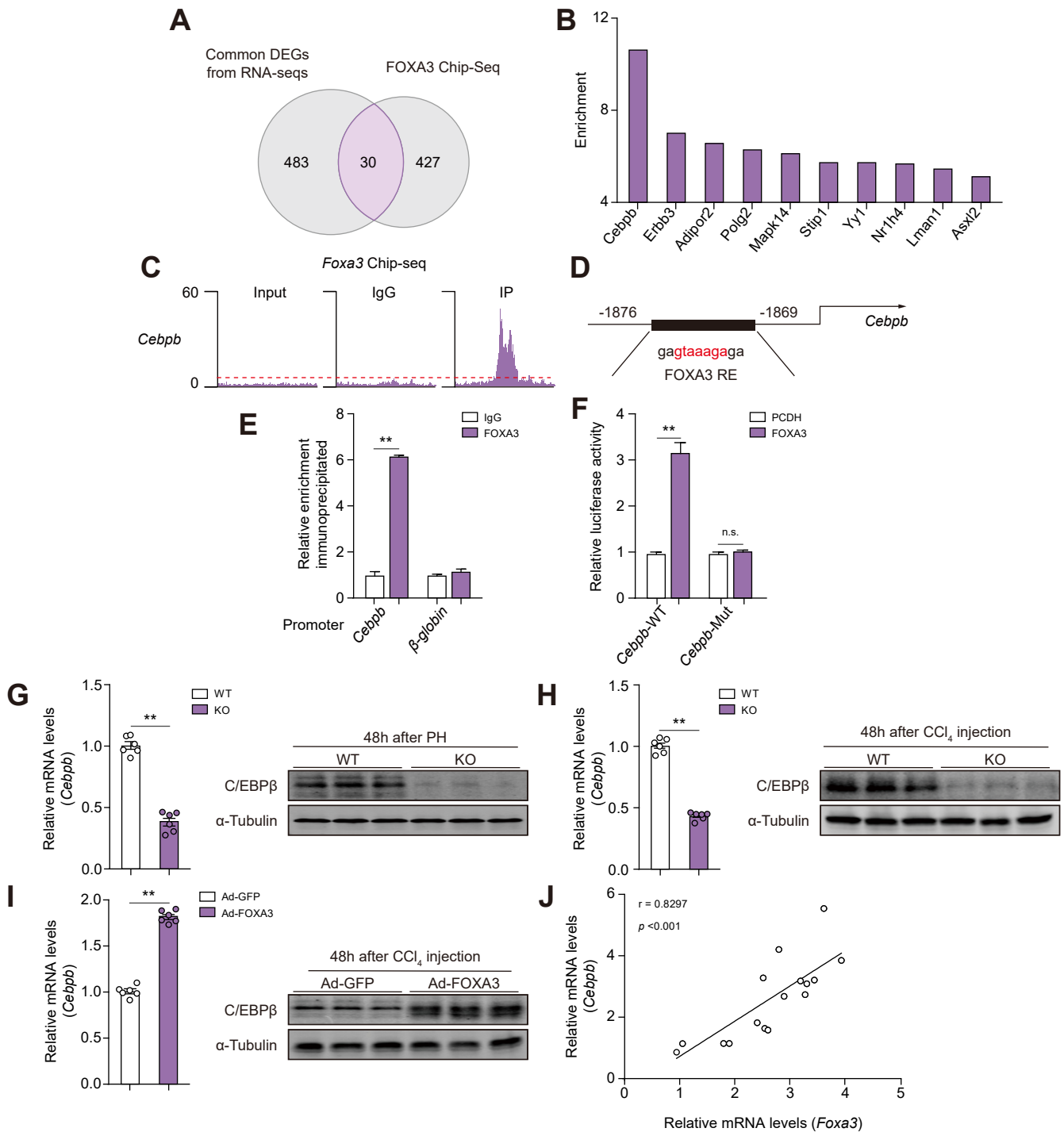


Fig. 5. FOXA3 regulates *Cebpb* transcription during liver regeneration. (A) Venn diagram illustrating overlap between 513 common DEGs (overlap of GSE133271, GSE70593, and GSE20427 as in Fig. 1A) and *Foxa3* ChIP-seq target genes in liver samples. (B) Top 10 genes enriched in *Foxa3* ChIP-seq data. (C) Visualisation of FOXA3 ChIP-seq data in the proximal region of the *Cebpb* promoter. (D) Putative FOXA-responsive element on the *Cebpb* promoter. (E) Confirmation of FOXA3 binding within the predicted *Foxa3* binding region on the *Cebpb* promoter by ChIP assay in AML12 cells ($n = 3$). (F) Luciferase activity of a WT *Cebpb* promoter (*Cebpb*-Luc) or a mutant-*Cebpb* reporter (*Cebpb*-Mut-Luc) containing a deletion of the *Foxa3*-responsive element in AML12 cells transiently expressing either vector (PCDH) or FOXA3. (G–I) *Cebpb* mRNA and protein levels were determined 48 h after PH in WT and FOXA3 KO mice (G), 48 h after CCl_4 injection in WT and FOXA3 KO mice, and (H) 48 h after CCl_4 injection in GFP/FOXA3 overexpression mice (I). (J) Pearson correlation analysis between normalised *Cebpb* mRNA levels and *Foxa3* mRNA levels in mice livers ($n = 18$). Data are presented as mean \pm SEM. Significance was determined using the Student two-tailed t test. * $p < 0.05$, ** $p < 0.01$, as indicated. $n = 6$ per group. AML12, alpha mouse liver 12; CCl_4 , carbon tetrachloride; ChIP-seq, chromatin immunoprecipitation sequencing; DEG, differentially expressed gene; FOXA, forkhead box A; FOXA3, forkhead box protein A3; GFP, green fluorescent protein; KO, knockout; PH, partial hepatectomy; RNA-seq, RNA sequencing; WT, wild-type.

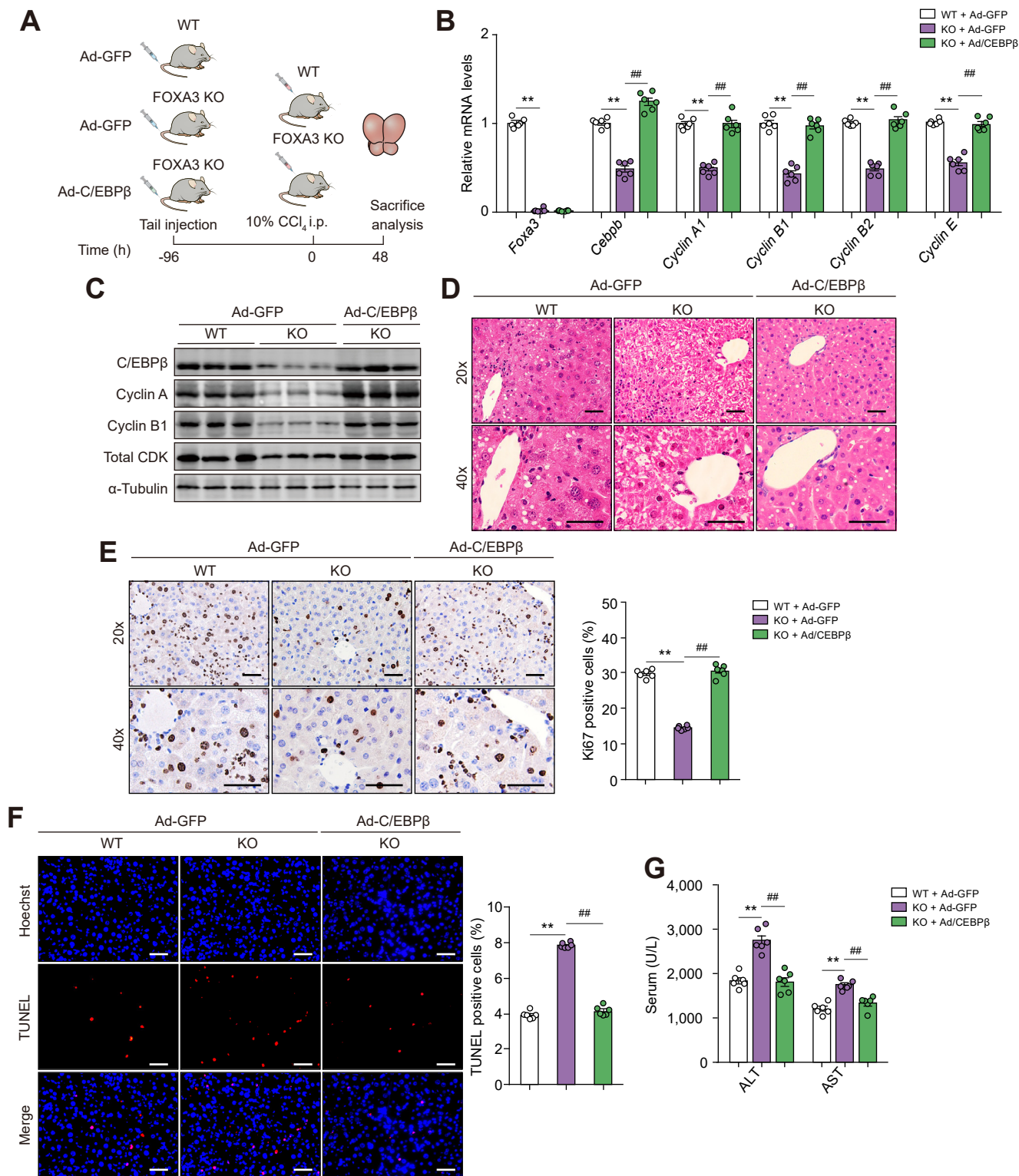


Fig. 6. C/EBPβ-mediated FOXA3 deficiency caused mitotic defects and apoptosis in hepatocytes and liver injury in mice upon CCl₄ administration. (A) Four days after tail vein injection of Ad-GFP or Ad-C/EBPβ, WT or FOXA3 KO mice were treated with CCl₄ (1 ml/kg body weight, i.p.) for 48 h. (B) Hepatic expression of cell cycle genes 48 h after CCl₄ injection. (C) Immunoblot of proliferative proteins 48 h after CCl₄ injection. (D–F) Representative H&E staining (D), immunohistochemistry for Ki67 (E), and TUNEL staining (F), as well as quantification 48 h after CCl₄ injection. (G) Serum ALT and AST levels 48 h after CCl₄ injection. Data are presented as mean ± SEM. Significance was determined using one-way ANOVA. *,# p < 0.05, **,## p < 0.01, as indicated. Scale bar, 50 μm. n = 6 per group. Ad, adenovirus; ALT, alanine aminotransferase; AST, aspartate aminotransferase; C/EBPβ, CCAAT/enhancer-binding protein beta; CCl₄, carbon tetrachloride; CCl₄, carbon tetrachloride; CDK, cyclin-dependent kinase; FOXA3, forkhead box protein A3; GFP, green fluorescent protein; KO, knockout; TUNEL, terminal deoxynucleotidyl transferase-mediated deoxyuridine triphosphate nick-end labelling; WT, wild-type.

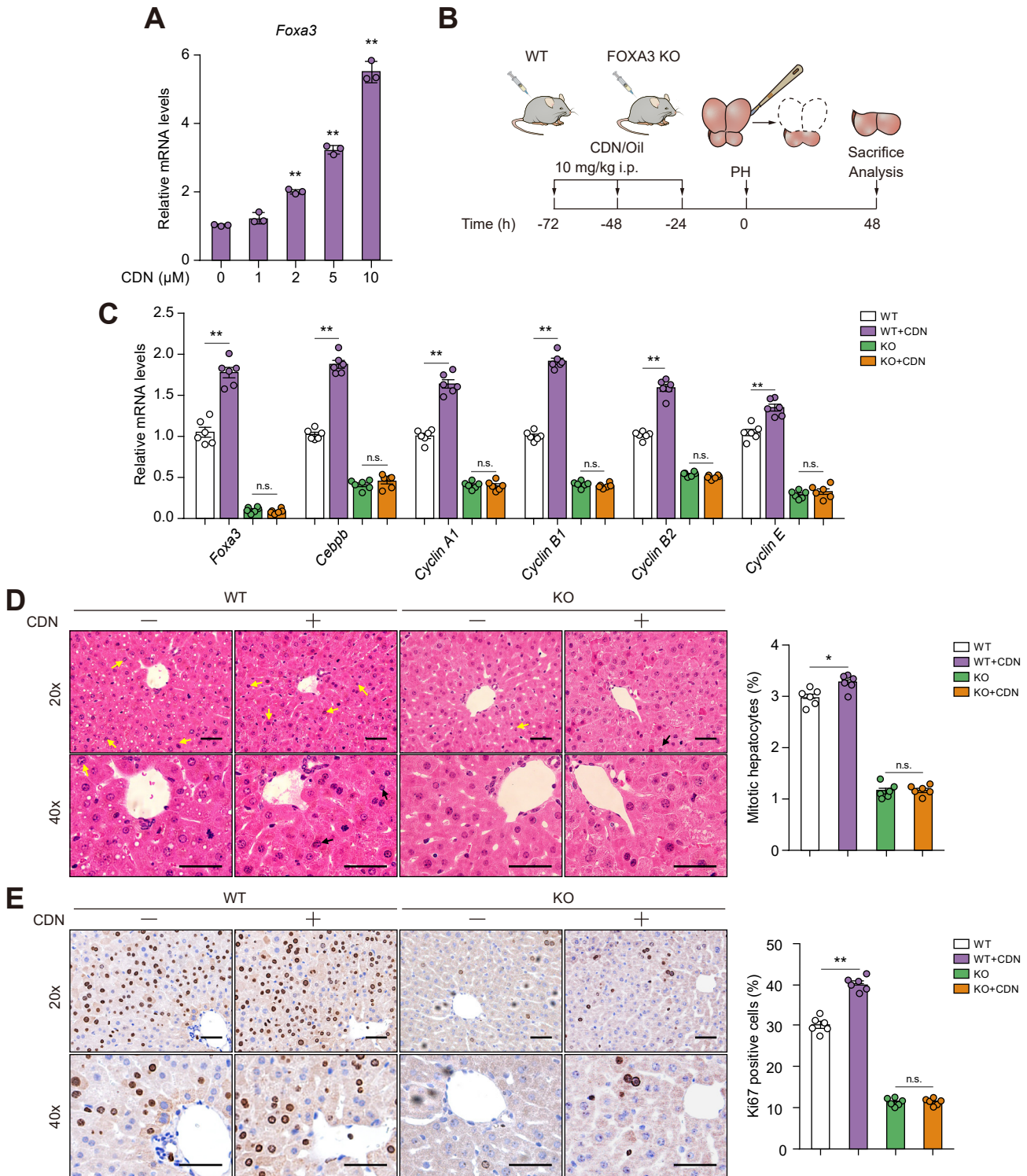


Fig. 7. Pharmacological induction of Foxa3 promotes hepatocyte proliferation after PH. (A) mRNA levels of Foxa3 in AML12 cells 36 h after treatment with different concentrations of CDN. (B) WT or FOXA3 KO mice were treated with olive oil or CDN (10 mg/kg body weight, dissolved in olive oil, i.p.) for 3 days (once per day), and then subjected to PH and sacrificed 48 h after PH. (C) Hepatic mRNA levels of Foxa3, Cebpb, and genes related to proliferation 48 h after PH. (D) Representative H&E staining of liver sections with mitotic hepatocytes quantified 48 h after PH. (E) Immunohistochemistry of liver sections for Ki67 48 h after PH, and Ki67-positive cells were quantified. Data are presented as mean \pm SEM. Significance was determined using the Student two-tailed *t* test. ***p* < 0.05, ****p* < 0.01, as indicated. Scale bar, 50 μm . *n* = 6 per group. AML12, alpha mouse liver 12; CDN, cardamomin; forkhead box protein A3; KO, knockout; PH, partial hepatectomy; WT, wild-type.

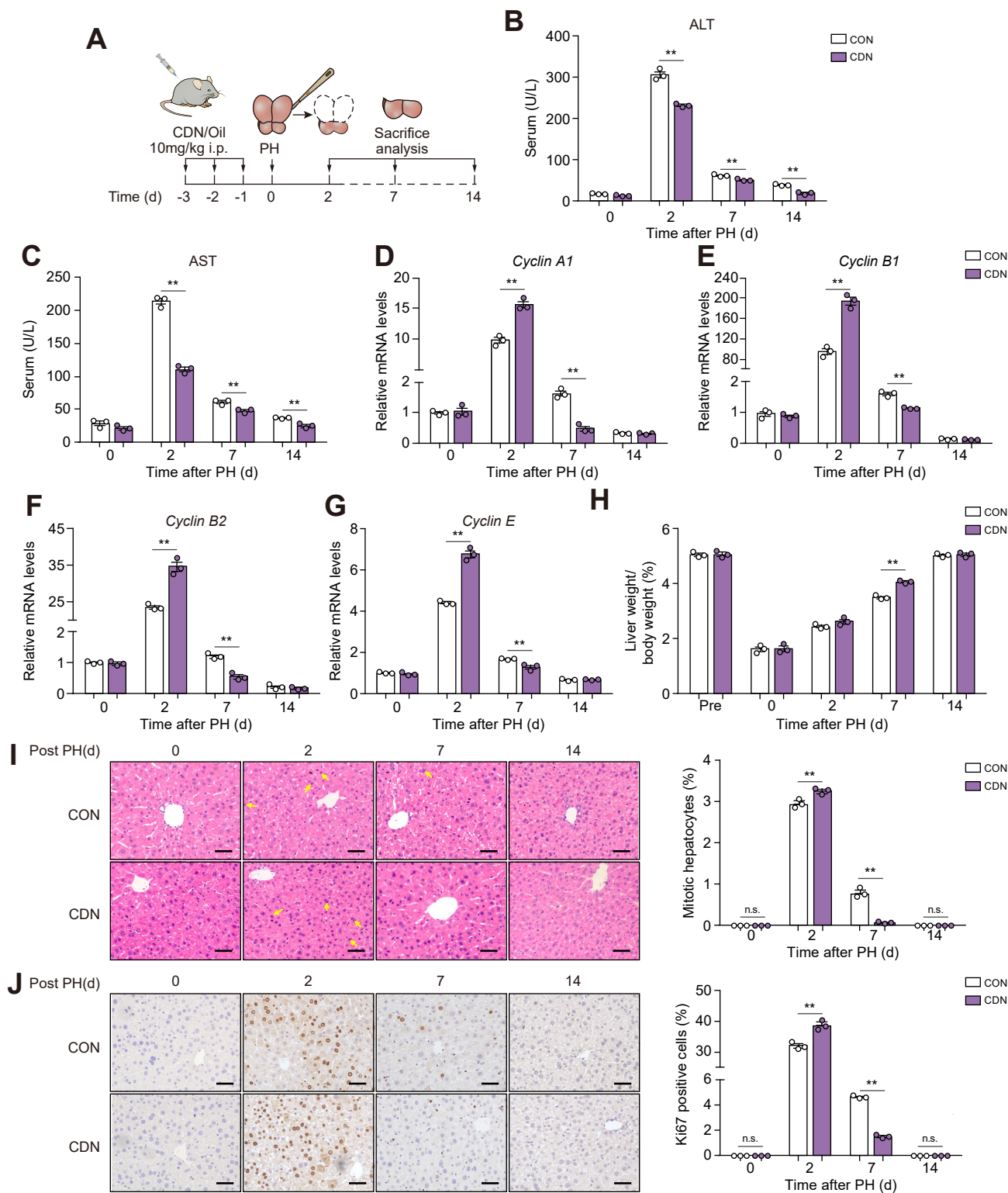


Fig. 8. CDN promotes liver regeneration without affecting termination after PH. (A) C57BL/6 mice were treated with olive oil (CON) or CDN (10 mg/kg body weight, dissolved in olive oil, i.p.) for 3 days (once each day), and then subjected to PH and sacrificed 0, 2, 7, and 14 days after PH. (B, C) Serum ALT and AST levels. (D–G) Expression of hepatic cyclin genes. (H) Restoration of liver mass. (I) Representative H&E staining of liver sections and quantification of mitotic hepatocytes. (J) Immunohistochemistry of liver sections for Ki67 and quantification. Scale bar, 50 μ m. Data are presented as mean \pm SEM. Significance was determined using the Student two-tailed *t* test. **p* < 0.05, ***p* < 0.01, as indicated. Scale bar, 50 μ m. ALT, alanine aminotransferase; AST, aspartate aminotransferase; CDN, cardamomin; CON, olive oil; PH, partial hepatectomy.

C/EBP β -mediated Foxa3 deficiency caused mitotic defects and apoptosis in hepatocytes and liver injury in mice upon CCl₄ administration

To further understand whether C/EBP β was downstream of Foxa3 for hepatocyte proliferation, we treated Foxa3-overexpressed hepatocytes with Cebpb siRNA (siCebpb). Because C/EBP β is also a TF, we confirmed that C/EBP β knockdown did not regulate Foxa3 levels (Fig. S8A) and found that C/EBP β knockdown blunted Foxa3-induced cell cycle gene expressions (Fig. S8B) and Ki67 levels (Fig. S8C), suggesting that C/EBP β silencing reversed the proliferative effect of Foxa3 in hepatocytes. Conversely, we further examined whether C/EBP β -mediated Foxa3 deficiency caused blunted proliferation and enhanced apoptosis of hepatocytes. C/EBP β overexpression did not change Foxa3 levels either (Fig. S9A). Subsequent *in vitro* analysis revealed that Foxa3 knockdown in hepatocytes reduced Cebpb levels, as well as expressions of cell cycle genes, which were reversed by Cebpb overexpression (Fig. S9A and B). Critically, replenishment of C/EBP β expression-rescued Foxa3 deficiency caused decreased Ki67 levels, defective cell mitosis, and increased apoptosis in hepatocytes (Fig. S9C and D).

Next, we used adenoviral-mediated gene delivery to examine *in vivo* function of C/EBP β in the Foxa3-regulated liver regeneration process. WT and Foxa3 KO mice were injected with Ad-GFP or Ad-C/EBP β via tail vein and treated with CCl₄ (Fig. 6A). As expected, Foxa3 KO mice characterised decreased Cebpb mRNA and protein levels in the liver, which were rescued by Ad-C/EBP β injection without affecting Foxa3 levels (Fig. 6B). Importantly, C/EBP β restored impaired hepatocyte proliferation and advanced liver injury in CCl₄-treated Foxa3 KO mice to degrees similar to those observed in WT mice, as evidenced by enhanced cell cycle gene expressions (Fig. 6B and C), attenuated lobular necrosis (Fig. 6D), increased Ki67-positive cells and mitotic hepatocytes (Fig. 6E and Fig. S9E), reduced serum ALT and AST levels (Fig. 6G), and decreased apoptotic cells (Fig. 6F) in Ad-C/EBP β Foxa3 KO mice. Collectively, these data suggested that C/EBP β is the downstream effector of Foxa3 for restoration of defective cell proliferation and alleviation of hepatocytes injury both *in vitro* and *in vivo*.

Pharmacological induction of Foxa3 promotes hepatocyte proliferation without affecting termination after PH

Based on our findings that the Foxa3-C/EBP β transcriptional axis enhanced cell proliferation for liver regeneration in scenarios of PH or CCl₄ administration, we then set out to examine whether pharmacological activation of this regulatory pathway could enhance liver regeneration. We constructed Foxa3 promoter reporter and screened the transactivation capability of 780 nature compounds on Foxa3 transcription. We identified CDN, the active gradient of *Alpinia katsumadai*, as a top Foxa3 transcriptional inducer (Table S6). In AML12 cells, CDN dose-dependently increased Foxa3 mRNA levels, without affecting cell survival rate (Fig. 7A and Fig. S10A). CDN also induced Cebpb expression, which was dependent on CDN induction on Foxa3, as CDN-induced Cebpb increase was blunted by Foxa3 knockdown (Fig. S10B and C). Consistent with our *in vitro* and *in vivo* data of the Foxa3 function on liver regeneration, we found that, as a Foxa3 transcription inducer, CDN could promote liver regeneration as shown by enhanced cell cycle gene programmes and Ki67 levels in CDN-treated hepatocytes, whereas Foxa3 knockdown via siFoxa3 abrogated these effects (Fig. S10D and E). We then tested the *in vivo* effects of CDN by pretreating WT and Foxa3 KO mice with CDN and then subjected them to PH (Fig. 7B). CDN treatment enhanced FOXA3 mRNA and protein levels before

mice were subjected to PH (Fig. S11A and B) but did not induce liver weights and cyclin gene expressions in mice, suggesting Foxa3-induced hepatocyte proliferation requires stimulus of regeneration (Fig. S11C and D). As expected, CDN treatment induced Foxa3 and Cebpb levels in WT mice but not in Foxa3 KO mice 48 h after PH (Fig. 7C). Importantly, CDN-treated WT mice showed improved liver repairment compared with control WT mice 2 days after PH, as shown by increased cell cycle genes and hepatocyte mitosis and proliferation, whereas these benefits of CDN were lost in Foxa3 KO mice (Fig. 7C-E and Fig. S10G). Overall, these data suggested that CDN accelerated liver regeneration after PH via modulating Foxa3 levels.

As uncontrolled cell proliferation is a prelude to carcinogenesis,⁴⁷ we investigated whether CDN affected termination of liver regeneration after PH. Mice were pretreated with CDN and then underwent PH. We sacrificed mice 0, 2, 7, and 14 days after PH to observe the effects of CDN on liver regeneration and termination (Fig. 8A). CDN treatment had no impact on liver weights in normal mice, as shown by the similar liver/body weight ratio between mice treated with or without CDN before PH (Fig. 8H). Consistent with previous observation, CDN treatment ameliorated liver damage along the regeneration process, as demonstrated by the overall decreased ALT and AST levels in CDN-treated mice (Fig. 8B and C). Notably, compared with controls, the CDN-treated group featured expedited liver repairment, as demonstrated by enhanced cell cycle gene programmes and elevated hepatocyte mitosis/proliferation 2 days after PH (Fig. 8D-G, I, and J, and Fig. S11E), which possibly led to the enhanced liver mass restoration (Fig. 8H) and an earlier tune-down of regeneration in CDN-treated mice 7 days post PH (Fig. 8D-G, I, and J, and Fig. S11E).

Critically, 14 days after PH, when liver regeneration is usually at its end,^{3-6,48} there is no further liver growth in CDN-treated mice, as both the control and CDN-treated groups reached liver sizes similar to those in the pre-PH stage, and both have comparable liver mass and molecular parameters (Fig. 8H-J and Fig. S11E), suggesting the safety of CDN administration. Overall, these data suggested that CDN promotes hepatocyte proliferation and liver mass restoration after PH without interfering with the normal termination of liver regeneration.

It has been shown that TFs Foxa3, Hnf1 α , and Gata4 activate p53 signalling during hepatic conversion from fibroblasts.⁴⁹ Considering that p53 is a key tumour suppressor for proliferation arrest, we examined p53 levels and found that both p53 mRNA and protein levels were increased by CDN at the late stage of hepatocyte proliferation in PH (Fig. S11F and G). Given that Foxa3 has been shown to serve as a pioneer factor to open compact chromatin and facilitate gene transcriptional activation, we performed a ChIP assay at the late stage of liver regeneration (Day 7) of PH to examine the occupancy of Foxa3 and H3K9 acetylation (H3K9ac) on p53 promoters. Consistently with enhanced p53 levels, we found Foxa3 occupancy and H3K9ac modification on p53 promoters, which were further enhanced by CDN treatment (Fig. S11H), suggesting that CDN may promote Foxa3-induced p53 activation at the late stage of liver regeneration possibly via chromatin remodelling to engage the normal regeneration termination after PH.

Discussion

In this study, through combined analysis of RNA-seq datasets and scRNA-seq data, we identified that Foxa3 as a TF plays a

potentially important role in hepatocyte proliferation and liver regeneration. Foxa3 levels were induced upon manipulations that enhanced liver regeneration, including PH and CCl₄-induced acute liver injury. Consistently, after PH and CCl₄ treatment, Foxa3 KO mice showed impaired hepatocyte proliferation and increased liver damage, whereas Foxa3 overexpression in mice livers characterised opposite phenotypes. Mechanistically, we found that Foxa3 binds to the C/EBP β promoter and trans-activates its transcription, thus regulating cell cycle genes, cell proliferation, and apoptosis. For translational purposes, we screened a lead compound CDN as a potent Foxa3 inducer and found that it promotes hepatocyte proliferation both *in vitro* and *in vivo* through its activation on Foxa3 expression without interfering with liver regeneration termination.

Through combined data analysis, aside from Foxa3, we also identified five other TFs, namely, Prox1, Stat3, Ctnnb1, Nfib, and Smarca2, that may play potential roles in hepatocyte proliferation during liver regeneration. Our screen results are supported by previous studies. For example, STAT3 has been reported to be critical for liver regeneration as activation of the IL-6–Stat3 pathway is one of the most important events to promote hepatocyte proliferation.^{4–6,32} Meanwhile, hepatocyte-specific KO of Ctnnb1 is shown to reduce cyclin gene expressions and delayed regeneration,⁵⁰ whereas Nfib, Ctnnb1, and Smarca2 were reported to promote cell proliferation in various cancer cells.^{51–53} Of note, we found that Prox1, a molecule required for hepatocyte migration during liver development,⁵⁴ features dominant expression in hepatocytes and cholangiocytes in a fashion similar to Foxa3, although with a lesser expression level. Interestingly, it has been shown that combined transduction of PROX1 and Foxa3, along with ATF5, Foxa2, and HNF4A, could efficiently convert human fibroblasts into hepatocyte-like cells.⁵⁵ However, PROX1 has been shown to promote HCC development and invasiveness through the Wnt/ β -catenin signalling cascade.³⁸ By contrast, HNF3 γ (Foxa3) is reported to promote differentiation of HCC cells, and its level is reversely correlated with HCC malignancy,²⁸ which renders Foxa3 a more suitable candidate for enhanced liver regeneration and avoids side effects such as carcinogenesis. Notably, we found that Foxa3 promotes liver regeneration, whereas previous studies of its role in cancer indicated that Foxa3 suppresses carcinogenesis. This may be as a result of the largely different regulatory network between liver regeneration and cancer development, which are two distinct physiological events activated by different pathological cues. For example, liver regeneration is normally activated by massive liver damage, and this proliferative process is strictly controlled and subdued after adequate repairment, whereas cancer development is impacted by various events including cancer initiation, growth, and metastasis. As a factor of versatile function, Foxa3 may play different roles in these different scenarios. Future work on the exact roles of Stat3, Ctnnb1, Nfib, and Smarca2 in liver regeneration, as well as the different regulatory network of Foxa3 and PROX1, may provide more insights.

Compared with its family members Foxa1 and Foxa2, which have been shown to be required for liver development, Foxa3 is dispensable for foetus liver formation as Foxa3 KO mice are viable and show no obvious defect.²¹ Recently, we and others have unravelled important roles of Foxa3 in energy metabolism. For example, Foxa3 is induced in adipose tissue under a high-fat-diet regimen and glucocorticoid treatment and during ageing, and it increases Ppar γ while inhibiting Pgc1 α transcriptions for energy hoarding.^{19,24} In addition, Foxa3 is induced in liver under

endoplasmic reticulum stress and regulates lipid homeostasis.²⁵ Foxa3 also maintains glucose homeostasis by regulating hepatic Glut2 expression during prolonged fast.²⁶ In the present study, we provided strong evidence that Foxa3 promotes hepatocyte proliferation during liver regeneration. Consistently, using a hydrodynamic screen system in a hereditary tyrosinaemia mice model, Wangenstein *et al.*⁵⁶ screened 43 potential candidates and indicated that Foxa3 is among top candidates for liver regeneration. In our study, we further demonstrated with genetic and adenovirus-manipulated mice models that Foxa3 is critical for liver regeneration through its direct regulation on C/EBP β . Although Foxa1 and Foxa2 belong to the same family with Foxa3, previous parallel genetic screen suggested that neither Foxa1 or Foxa2 has any effects on liver repopulation.⁵⁶ This functional difference may be attributable to the significantly lower Foxa1 and Foxa2 levels than Foxa3 levels in the adult liver, as shown by our scRNA-seq analysis. It is possible that, unique to Foxa1 and Foxa2, Foxa3 is dispensable for liver development but in turn plays a major role in maintaining normal functions of the adult liver; thus, it endows its uniqueness in suppressing HCC development. For instance, Foxa3 is one of the key hepatocyte nuclear factors that could reprogramme various types of cells, including hepatic myofibroblasts, human fibroblasts, and spleen fibroblasts, into functional and expandable hepatocyte-like cells.^{55,57,58} Consistent with this idea, it is reported that the HNF3 γ (Foxa3) level was downregulated in patients with HCC and inversely correlated with HCC malignancy and patient survival.²⁸ In addition, HNF3 γ (Foxa3) overexpression led to suppression of HCC growth and sensitised HCC cells to sorafenib-induced growth inhibition and cell apoptosis.²⁸ Aside from its role as a TF, Foxa3 is also an important pioneer factor that functions by opening up chromatin to facilitate gene trans-activation. For example, we demonstrated previously that Foxa3 is downstream of the glucocorticoid receptor signalling pathway and facilitates the binding of the glucocorticoid receptor to its target gene promoters in fat tissues.²⁴ Intriguingly, in this study, we found Foxa3 binding and histone acetylation on the P53 promoter at the late stage of liver regeneration after PH, which is further increased by Foxa3-induced CDN administration. P53, as a classic tumour suppressor, thus effectively mediates the proper termination of hepatocyte proliferation and liver regeneration to control the potentially harmful proliferating process if left unrestrained. This may also underline the ability of Foxa3 to suppress HCC development and overall suggests that Foxa3 may be a safe and effective therapeutic target for liver regeneration. It has to be noted that although we mainly intended to study the contribution of Foxa3 in hepatocytes, we cannot fully exclude the possibility of Foxa3 in other cell types (*i.e.* cholangiocytes and stem cells) contributing to the process, especially under the scenario of chronic liver diseases where hepatocytes undergo profound proliferative senescence.

Mechanistically, we demonstrated that Cebpb is the direct transcriptional target gene of Foxa3 and mediates its enhancement of hepatocyte proliferation. It has been well accepted that C/EBP β plays an important role in liver regeneration. C/EBP β levels are increased in the liver during the period of cell proliferation, which contributes to HGF-induced replication of mice hepatocytes.^{40,59} Strikingly, liver DNA synthesis in C/EBP β KO mice was decreased to 25% that in normal mice after PH, accompanied with dramatically reduced expressions of Cyclin B and Cyclin E.⁵⁹ In addition, C/EBP β and HDAC1 form complexes to epigenetically control key regulators, that is, Ki67, to

orchestrate hepatocyte mitosis and liver proliferation.⁶⁰ These functions of C/EBP β are in consistent with the defective hepatocyte proliferation of Foxa3 KO mice upon acute liver injury mainly as a result of impaired Ki67 and Cyclin expressions, which were largely rescued by C/EBP β replenishing in Foxa3 KO mice.

CDN is a naturally occurring chalcone isolated from the seeds of *Alpinia katsumadai*, a medical herb that has been widely used to treat digestive system-related diseases, and recently, it has also been shown to exhibit anti-inflammatory, anti-cancer, anti-oxidative, and vasorelaxant activities.^{61–63} By screening natural compounds, we identified CDN as a potent inducer of Foxa3. CDN treatment enhanced liver regeneration after PH, but CDN administration could not rescue the suppressed liver regeneration of Foxa3 KO mice upon PH, indicating that the effects of CDN is dependent on Foxa3. Previous studies found that CDN reduces acetaminophen-induced acute liver injury and ischaemia-reperfusion injury in mice,^{64,65} and it has anti-proliferative effects and pro-apoptotic action on hepatoma cells.⁶² These characters of CDN may be explained by its effective transactivation on Foxa3, which we and others have shown could promote liver regeneration while inhibiting HCC progression. Importantly, although CDN promotes liver regeneration, we found that it does not interfere with the normal termination of liver repair, possibly through a role of Foxa3 on P53 modification and activation. As uncontrolled cell proliferation is a prelude to carcinogenesis, our

findings would largely relieve the concern that CDN administration may cause unrestrained proliferation and lead to hepatoma. Thus, CDN is a promising lead compound for adjuvant therapy in the treatment of primary liver cancer with PH or acute liver injury with liver transplantation, although preclinical studies and further studies for structural optimising to find more ideal CDN derivatives are warranted.

In the study, we assessed the liver weight and hepatocyte proliferation in healthy mice with Foxa3 overexpression by AAV-TBG-Foxa3 or CDN treatment without CCl₄ injection or PH. The results showed that there was no difference in liver weights and cyclin gene expressions, suggesting that overexpression of Foxa3 does not cause hepatomegaly or hepatocyte proliferation in healthy livers. On the one hand, the induction of Foxa3–Cebpb axis initiation may need a further stimulus, that is, the stress signals present in liver regeneration. On the other hand, we have reported that Foxa3 also induces p53, which is well known for proliferation arrest, and thus may reach regulatory balance on hepatocyte proliferation.

In summary, our work demonstrated a critical role of Foxa3 in hepatocyte proliferation and liver regeneration through its transactivation of C/EBP β , and identified a natural compound, CDN, as a potent Foxa3 transcriptional activator. Avenues to promote Foxa3 levels, including CDN, may be beneficial for treating liver injury.

Abbreviations

AAV, adeno-associated virus; Ad, adenovirus; ALT, alanine aminotransferase; AML12, alpha mouse liver 12; AST, aspartate aminotransferase; C/EBP, CCAAT/enhancer-binding protein; C/EBP β , CCAAT/enhancer-binding protein beta; CCl₄, carbon tetrachloride; CDK, cyclin-dependent kinase; CDN, cardamonin; ChIP, chromatin immunoprecipitation; ChIP-seq, chromatin immunoprecipitation sequencing; DEG, differentially expressed gene; EGF, epidermal growth factor; HGF, hepatocyte growth factor; FOXA3, forkhead box protein A3; GEO, Gene Expression Omnibus; GO, gene ontology; H3K9ac, H3K9 acetylation; HCC, hepatocellular carcinoma; HNF3, hepatocyte nuclear factor 3; HNF3 γ , hepatocyte nuclear factor 3 γ ; HNF1A, hepatocyte nuclear factor 1A; HNF4A, hepatocyte nuclear factor 4A; IGV, Integrative Genomic Viewer; KO, knockout; NASH, non-alcoholic steatohepatitis; PH, partial hepatectomy; RNA-seq, RNA sequencing; scRNA-seq, single-cell RNA sequencing; siRNA, small interfering RNA; STAT3, signal transducer and activator of transcription 3; t-SNE, t-distributed stochastic neighbour embedding; TBG, thyroxine-binding globulin; TUNEL, terminal deoxynucleotidyl transferase-mediated deoxyuridine triphosphate nick-end labelling; WT, wild-type.

Financial support

This project is supported by funds from the National Key Research and Development Program of China (2019YFA0904500); the National Natural Science Foundation of China (32022034, 32222024, 32271224, 32071148, and 81970751); the National Science Foundation of Chongqing, China (CSTB2022NSCQ-JQX0033); the Science and Technology Commission of Shanghai Municipality (21140904300, 22ZR1421200); the Fundamental Research Funds for the Central Universities, and ECNU Public Platform for Innovation (011) and the Instruments Sharing Platform of School of Life Sciences. We also thank Professor Li Yu (Chinese Academy of Sciences) for technique supports and helpful discussions.

Conflicts of interest

The authors declare no competing interests.

Please refer to the accompanying ICMJE disclosure forms for further details.

Authors' contributions

Devised and supervised the project: LX, XM, MZ. Performed biochemical and cellular experiments: GL, MG, MM, DW, YZ, YG, YC, ZX. Established animal models: GL, LZ, MG, ZZ, MM, JW, SL. Participated in animal studies: YC, SL, YZ. Performed RNA-seq and single-cell RNA-seq analysis: MG, ZZ, YL, CL, JQ, YL. Provided clinical liver samples: YH, WL, MZ. Wrote and edited the manuscript: GL, XM, LX.

Data availability statement

The data supporting the findings of this study are available upon request.

Supplementary data

Supplementary data to this article can be found online at <https://doi.org/10.1016/j.jhepr.2023.100906>.

References

Author names in bold designate shared co-first authorship

- [1] Kietzmann T. Metabolic zonation of the liver: the oxygen gradient revisited. *Redox Biol* 2017;11:622–630.
- [2] **Lonardo A, Byrne CD, Caldwell SH, Cortez-Pinto H, Targher G.** Global epidemiology of nonalcoholic fatty liver disease: meta-analytic assessment of prevalence, incidence, and outcomes. *Hepatology* 2016;64:1388–1389.
- [3] **Michalopoulos GK.** Hepatostat: liver regeneration and normal liver tissue maintenance. *Hepatology* 2017;65(4):1384–1392.
- [4] **Michalopoulos GK.** Liver regeneration after partial hepatectomy: critical analysis of mechanistic dilemmas. *Am J Pathol* 2010;176:2–13.
- [5] **Forbes SJ, Newsome PN.** Liver regeneration – mechanisms and models to clinical application. *Nat Rev Gastroenterol Hepatol* 2016;13:473–485.
- [6] **Michalopoulos GK, Bhushan B.** Liver regeneration: biological and pathological mechanisms and implications. *Nat Rev Gastroenterol Hepatol* 2021;18:40–55.
- [7] **Marshall A, Rushbrook S, Davies SE, Morris LS, Scott IS, Vowler SL, et al.** Relation between hepatocyte G1 arrest, impaired hepatic regeneration, and fibrosis in chronic hepatitis C virus infection. *Gastroenterology*

- 2005;128:33–42.
- [8] Cray GS, Albrecht JH. Expression of cyclin-dependent kinase inhibitor p21 in human liver. *Hepatology* 1998;28:738–743.
 - [9] Williams MJ, Clouston AD, Forbes SJ. Links between hepatic fibrosis, ductular reaction, and progenitor cell expansion. *Gastroenterology* 2014;146:349–356.
 - [10] Eleazar JA, Memeo L, Jhang JS, Mansukhani MM, Chin S, Park SM, et al. Progenitor cell expansion: an important source of hepatocyte regeneration in chronic hepatitis. *J Hepatol* 2004;41:983–991.
 - [11] Rudolph KL, Chang S, Millard M, Schreiber-Agus N, DePinho RA. Inhibition of experimental liver cirrhosis in mice by telomerase gene delivery. *Science* 2000;287:1253–1258.
 - [12] Nobili V, Carpino G, Alisi A, Franchitto A, Alpini G, De Vito R, et al. Hepatic progenitor cells activation, fibrosis, and adipokines production in pediatric nonalcoholic fatty liver disease. *Hepatology* 2016;56:2142–2153.
 - [13] Raven A, Lu WY, Man TY, Ferreira-Gonzalez S, O'Duibhir E, Dwyer BJ, et al. Cholangiocytes act as facultative liver stem cells during impaired hepatocyte regeneration. *Nature* 2017;547:350–354.
 - [14] Lu WY, Bird TG, Boulter L, Tsuchiya A, Cole AM, Hay T, et al. Hepatic progenitor cells of biliary origin with liver repopulation capacity. *Nat Cell Biol* 2015;17:971–983.
 - [15] Petrowsky H, Fritsch R, Guckenberger M, De Oliveira ML, Dutkowski P, Clavien PA. Modern therapeutic approaches for the treatment of malignant liver tumours. *Nat Rev Gastroenterol Hepatol* 2020;17:755–772.
 - [16] Du Y, Zhang W, Qiu H, Xiao C, Shi J, Reid LM, et al. Mouse models of liver parenchyma injuries and regeneration. *Front Cell Dev Biol* 2022;10:903740.
 - [17] Charni M, Aloni-Grinstein R, Molchadsky A, Rotter V. p53 on the cross-road between regeneration and cancer. *Cell Death Differ* 2017;24:8–14.
 - [18] Friedman JR, Kaestner KH. The Foxa family of transcription factors in development and metabolism. *Cell Mol Life Sci* 2006;63:2317–2328.
 - [19] Ma X, Xu L, Gavrilova O, Mueller E. Role of forkhead box protein A3 in age-associated metabolic decline. *Proc Natl Acad Sci U S A* 2014;111:14289–14294.
 - [20] Lee CS, Friedman JR, Fulmer JT, Kaestner KH. The initiation of liver development is dependent on Foxa transcription factors. *Nature* 2005;435:944–947.
 - [21] Kaestner KH, Hiemisch H, Schütz G. Targeted disruption of the gene encoding hepatocyte nuclear factor 3 γ results in reduced transcription of hepatocyte-specific genes. *Mol Cell Biol* 1998;18:4245–4251.
 - [22] Kaestner KH, Hiemisch H, Luckow B, Schütz G. The HNF-3 gene family of transcription factors in mice: gene structure, cDNA sequence, and mRNA distribution. *Genomics* 1994;20:377–385.
 - [23] Reizel Y, Morgan A, Gao L, Lan Y, Manduchi E, Waite EL, et al. Collapse of the hepatic gene regulatory network in the absence of FoxA factors. *Genes Dev* 2020;34:1039–1050.
 - [24] Ma X, Xu L, Mueller E. Forkhead box A3 mediates glucocorticoid receptor function in adipose tissue. *Proc Natl Acad Sci U S A* 2016;113:3377–3382.
 - [25] Liu C, Zhou B, Meng M, Zhao W, Wang D, Yuan Y, et al. FOXA3 induction under endoplasmic reticulum stress contributes to non-alcoholic fatty liver disease. *J Hepatol* 2021;75:150–162.
 - [26] Shen W, Searce LM, Brestelli JE, Sund NJ, Kaestner KH. Foxa3 (hepatocyte nuclear factor 3 γ) is required for the regulation of hepatic GLUT2 expression and the maintenance of glucose homeostasis during a prolonged fast. *J Biol Chem* 2001;276:42812–42817.
 - [27] Li Y, Xu Y, Jadhav K, Zhu Y, Yin L, Zhang Y. Hepatic forkhead box protein A3 regulates ApoA-I (apolipoprotein A-I) expression, cholesterol efflux, and atherogenesis. *Arterioscler Thromb Vasc Biol* 2019;39:1574–1587.
 - [28] Zhou T, Li S, Xiang D, Liu J, Sun W, Cui X, et al. m6A RNA methylation-mediated HNF3 γ reduction renders hepatocellular carcinoma dedifferentiation and sorafenib resistance. *Signal Transduct Target Ther* 2020;5:296.
 - [29] Cheng Z, He Z, Cai Y, Zhang C, Fu G, Li H, et al. Conversion of hepatoma cells to hepatocyte-like cells by defined hepatocyte nuclear factors. *Cell Res* 2019;29:124–135.
 - [30] Xu L, Panel V, Ma X, Du C, Hugendubler L, Gavrilova O, et al. The winged helix transcription factor Foxa3 regulates adipocyte differentiation and depot-selective fat tissue expansion. *Mol Cell Biol* 2013;33:3392–3399.
 - [31] Mitchell C, Willenbring H. A reproducible and well-tolerated method for 2/3 partial hepatectomy in mice. *Nat Protoc* 2008;3:1167–1170.
 - [32] Hu Z, Han Y, Liu Y, Zhao Z, Ma F, Cui A, et al. CREBZF as a key regulator of STAT3 pathway in the control of liver regeneration in mice. *Hepatology* 2020;71:1421–1436.
 - [33] Wei Y, Wang YG, Jia Y, Li L, Yoon J, Zhang S, et al. Liver homeostasis is maintained by midlobular zone 2 hepatocytes. *Science* 2021;371:eabb1625.
 - [34] Korsunsky I, Millard N, Fan J, Slowikowski K, Zhang F, Wei K, et al. Fast, sensitive and accurate integration of single-cell data with Harmony. *Nat Methods* 2019;16:1289–1296.
 - [35] Hao Y, Hao S, Andersen-Nissen E, Mauck 3rd WM, Zheng S, Butler A, et al. Integrated analysis of multimodal single-cell data. *Cell* 2021;184:3573–3587.e29.
 - [36] Xiong X, Kuang H, Ansari S, Liu T, Gong J, Wang S, et al. Landscape of intercellular crosstalk in healthy and NASH liver revealed by single-cell secretome gene analysis. *Mol Cell* 2019;75(3):644–660.e5.
 - [37] Sun X, Wu J, Liu L, Chen Y, Tang Y, Liu S, et al. Transcriptional switch of hepatocytes initiates macrophage recruitment and T-cell suppression in endotoxemia. *J Hepatol* 2022;77:436–452.
 - [38] Liu Y, Ye X, Zhang JB, Ouyang H, Shen Z, Wu Y, et al. PROX1 promotes hepatocellular carcinoma proliferation and sorafenib resistance by enhancing β -catenin expression and nuclear translocation. *Oncogene* 2015;34:5524–5535.
 - [39] Isoda K, Koide H, Kojima M, Arita E, Ikkaku M, Higashiyama S, et al. Stimulation of hepatocyte survival and suppression of CCl $_4$ -induced liver injury by the adenovirally introduced C/EBP β gene. *Biochem Biophys Res Commun* 2005;329:182–187.
 - [40] Wang B, Gao C, Ponder KP. C/EBP β contributes to hepatocyte growth factor-induced replication of rodent hepatocytes. *J Hepatol* 2005;43:294–302.
 - [41] Meng Z, Wang Y, Wang L, Jin W, Liu N, Pan H, et al. FXR regulates liver repair after CCl $_4$ -induced toxic injury. *Mol Endocrinol* 2010;24:886–897.
 - [42] Cai P, Mao X, Zhao J, Nie L, Jiang Y, Yang Q, et al. Farnesoid X receptor is required for the redifferentiation of bipotential progenitor cells during biliary-mediated zebrafish liver regeneration. *Hepatology* 2021;74:3345–3361.
 - [43] Masson MJ, Collins LA, Carpenter LD, Graf ML, Ryan PM, Bourdi M, et al. Pathologic role of stressed-induced glucocorticoids in drug-induced liver injury in mice. *Biochem Biophys Res Commun* 2010;397:453–458.
 - [44] Shteyer E, Liao Y, Muglia LJ, Hruz PW, Rudnick DA. Disruption of hepatic adipogenesis is associated with impaired liver regeneration in mice. *Hepatology* 2004;40:1322–1332.
 - [45] Wu K, Ma L, Xu T, Cao J, Zhou C, Yu X, et al. Transcription factor YY1 ameliorates liver ischemia-reperfusion injury through modulating the miR-181a-5p/ESR1/ERBB2 axis. *Transplantation* 2023;107:878–889.
 - [46] Wang Q, Wei S, Li L, Qiu J, Zhou S, Shi C, et al. TGR5 deficiency aggravates hepatic ischemic/reperfusion injury via inhibiting SIRT3/FOXO3/HIF-1 α pathway. *Cell Death Discov* 2020;6:116.
 - [47] Otto T, Sicinski P. Cell cycle proteins as promising targets in cancer therapy. *Nat Rev Cancer* 2017;17:93–115.
 - [48] Kawaguchi T, Kodama T, Hikita H, Tanaka S, Shigekawa M, Nawa T, et al. Carbamazepine promotes liver regeneration and survival in mice. *J Hepatol* 2013;59:1239–1245.
 - [49] Ji S, Zhu L, Gao Y, Zhang X, Yan Y, Cen J, et al. Baf60b-mediated ATM-p53 activation blocks cell identity conversion by sensing chromatin opening. *Cell Res* 2017;27:642–656.
 - [50] Tan X, Behari J, Cieply B, Michalopoulos GK, Monga SP. Conditional deletion of beta-catenin reveals its role in liver growth and regeneration. *Gastroenterology* 2006;131:1561–1572.
 - [51] Zilli F, Marques Ramos P, Auf der Maur P, Jehanno C, Sethi A, Coissieux MM, et al. The NFIB-ERO1A axis promotes breast cancer metastatic colonization of disseminated tumour cells. *EMBO Mol Med* 2021;13:e13162.
 - [52] Zhang Y, Xu H, Cui G, Liang B, Chen X, Ko S, et al. β -Catenin sustains and is required for YES-associated protein oncogenic activity in cholangiocarcinoma. *Gastroenterology* 2022;163:481–494.
 - [53] Shen H, Powers N, Saini N, Comstock CES, Sharma A, Weaver K, et al. The SWI/SNF ATPase Brm is a gatekeeper of proliferative control in prostate cancer. *Cancer Res* 2008;68:10154–10162.
 - [54] Sosa-Pineda B, Wigle JT, Oliver G. Hepatocyte migration during liver development requires Prox1. *Nat Genet* 2000;25:254–255.
 - [55] Nakamori D, Akamine H, Takayama K, Sakurai F, Mizuguchi H. Direct conversion of human fibroblasts into hepatocyte-like cells by ATF5, PROX1, FOXA2, FOXA3, and HNF4A transduction. *Sci Rep* 2017;7:16675.
 - [56] Wangenstein KJ, Zhang S, Greenbaum LE, Kaestner KH. A genetic screen reveals Foxa3 and TNFR1 as key regulators of liver repopulation. *Genes Dev* 2015;29:904–909.
 - [57] Song G, Pacher M, Balakrishnan A, Yuan Q, Tsay HC, Yang D, et al. Direct reprogramming of hepatic myofibroblasts into hepatocytes in vivo attenuates liver fibrosis. *Cell Stem Cell* 2016;18:797–808.
 - [58] Liu C, Wang L, Xu M, Sun Y, Xing Z, Zhang J, et al. Reprogramming the spleen into a functioning ‘liver’ in vivo. *Gut* 2022;71:2325–2336.
 - [59] Greenbaum LE, Li W, Cressman DE, Peng Y, Ciliberto G, Poli V, et al. CCAAT enhancer-binding protein beta is required for normal hepatocyte

- proliferation in mice after partial hepatectomy. *J Clin Invest* 1998;102:996–1007.
- [60] Xia J, Zhou Y, Ji H, Wang Y, Wu Q, Bao J, et al. Loss of histone deacetylases 1 and 2 in hepatocytes impairs murine liver regeneration through Ki67 depletion. *Hepatology* 2013;58:2089–2098.
- [61] Peng YJ, Lu JW, Lee CH, Lee HS, Chu YH, Ho YJ, et al. Cardamonin attenuates inflammation and oxidative stress in interleukin-1 β -stimulated osteoarthritis chondrocyte through the Nrf2 pathway. *Antioxidants (Basel)* 2021;10:862.
- [62] Badroon NA, Abdul Majid N, Alshawsh MA. Antiproliferative and apoptotic effects of cardamonin against hepatocellular carcinoma HepG2 cells. *Nutrients* 2020;12:1757.
- [63] Wang ZT, Lau CW, Chan FL, Yao X, Chen ZY, He ZD, et al. Vasorelaxant effects of cardamonin and alpinetin from *Alpinia henryi* K. Schum. *J Cardiovasc Pharmacol* 2001;37:596–606.
- [64] Xu Q, Fan Y, Loo JJ, Liang Y, Sun X, Jia H, et al. Cardamonin reduces acetaminophen-induced acute liver injury in mice via activating autophagy and NFE2L2 signaling. *Front Pharmacol* 2020;11:601716.
- [65] Atef Y, El-Fayoumi HM, Abdel-Mottaleb Y, Mahmoud MF. Effect of cardamonin on hepatic ischemia reperfusion induced in rats: role of nitric oxide. *Eur J Pharmacol* 2017;815:446–453.